



**NAVAL  
POSTGRADUATE  
SCHOOL**

**MONTEREY, CALIFORNIA**

**THESIS**

**THE VIABILITY OF A METAMATERIAL SOLUTION FOR  
THE DEFENSE OF AN INCIDENT HIGH-ENERGY  
ELECTROMAGNETIC BEAM**

by

Alex B. Baynes

December 2010

Thesis Advisor: James H. Luscombe  
Thesis Co-Advisor: Clyde L. Scandrett

**Approved for public release; distribution is unlimited.**

THIS PAGE INTENTIONALLY LEFT BLANK

REPORT DOCUMENTATION PAGE		Form Approved OMB No. 0704-0188	
Public reporting burden for this collection of information is estimated to average 1 hour per response, including the time for reviewing instruction, searching existing data sources, gathering and maintaining the data needed, and completing and reviewing the collection of information. Send comments regarding this burden estimate or any other aspect of this collection of information, including suggestions for reducing this burden, to Washington headquarters Services, Directorate for Information Operations and Reports, 1215 Jefferson Davis Highway, Suite 1204, Arlington, VA 22202-4302, and to the Office of Management and Budget, Paperwork Reduction Project (0704-0188) Washington DC 20503.			
1. AGENCY USE ONLY (Leave blank)	2. REPORT DATE December 2010	3. REPORT TYPE AND DATES COVERED Master's Thesis	
4. TITLE AND SUBTITLE The Viability of a Metamaterial Solution for the Defense of an Incident High-Energy Electromagnetic Beam		5. FUNDING NUMBERS	
6. AUTHOR(S) Alex B. Baynes		8. PERFORMING ORGANIZATION REPORT NUMBER	
7. PERFORMING ORGANIZATION NAME(S) AND ADDRESS(ES) Naval Postgraduate School Monterey, CA 93943-5000		10. SPONSORING/MONITORING AGENCY REPORT NUMBER	
9. SPONSORING /MONITORING AGENCY NAME(S) AND ADDRESS(ES) N/A		11. SUPPLEMENTARY NOTES The views expressed in this thesis are those of the author and do not reflect the official policy or position of the Department of Defense or the U.S. Government.	
12a. DISTRIBUTION / AVAILABILITY STATEMENT Approved for public release; distribution is unlimited.		12b. DISTRIBUTION CODE	
13. ABSTRACT (maximum 200 words) Metamaterials have given rise to envisioning the design and engineering of materials through which light would be directed by design. The purpose of this thesis is to explore the idea of using transformational optics through the use of metamaterials as a way of defending against an incident electromagnetic beam. The theoretical and realistic viability of two possible proposed material solutions will be tested, through the use of the COMSOL Multiphysics software package.			
14. SUBJECT TERMS Counter-Directed Energy Weapons, Directed Energy Weapons, Metamaterials, Transformational Optics, Cloaking, Free Electron Laser, Anti-Ship Missile, Office of Naval Research			15. NUMBER OF PAGES 97
			16. PRICE CODE
17. SECURITY CLASSIFICATION OF REPORT Unclassified	18. SECURITY CLASSIFICATION OF THIS PAGE Unclassified	19. SECURITY CLASSIFICATION OF ABSTRACT Unclassified	20. LIMITATION OF ABSTRACT UU

NSN 7540-01-280-5500

Standard Form 298 (Rev. 2-89)  
Prescribed by ANSI Std. Z39-18

THIS PAGE INTENTIONALLY LEFT BLANK

Approved for public release; distribution is unlimited.

**THE VIABILITY OF A METAMATERIAL SOLUTION FOR THE DEFENSE OF  
AN INCIDENT HIGH-ENERGY ELECTROMAGNETIC BEAM**

Alex B. Baynes  
Lieutenant, United States Navy  
B.S., Cornell University, 2004

Submitted in partial fulfillment of the  
requirements for the degrees of

**MASTER OF SCIENCE IN PHYSICS  
and  
MASTER OF SCIENCE IN APPLIED MATHEMATICS**

from the

**NAVAL POSTGRADUATE SCHOOL  
DECEMBER 2010**

Author: Alex B. Baynes

Approved by: James H. Luscombe  
Thesis Advisor

Clyde L. Scandrett  
Co-Advisor

Andres Larraza  
Chairman, Department of Physics

Carlos F. Borges  
Chairman, Department of Applied Mathematics

THIS PAGE INTENTIONALLY LEFT BLANK

## **ABSTRACT**

Metamaterials have given rise to envisioning the design and engineering of materials through which light would be directed by design. The purpose of this thesis is to explore the idea of using transformational optics through the use of metamaterials as a way of defending against an incident electromagnetic beam. The theoretical and realistic viability of two possible proposed material solutions will be tested, through the use of the COMSOL Multiphysics software package.

THIS PAGE INTENTIONALLY LEFT BLANK



## TABLE OF CONTENTS

I.	INTRODUCTION .....	1
A.	DIRECTED ENERGY WEAPONS (DEW) .....	1
B.	FREE ELECTRON LASER (FEL) .....	1
1.	Background .....	2
2.	Navy FEL Relevance .....	3
C.	COUNTER-DIRECTED ENERGY WEAPONS (C-DEW) .....	7
1.	Navy Relevance .....	7
2.	Problem Description .....	7
II.	METAMATERIALS .....	11
A.	BACKGROUND .....	11
B.	PROPERTIES .....	13
C.	DESIGN AND MANUFACTURING .....	16
III.	TRANSFORMATIONAL OPTICS .....	17
A.	BACKGROUND .....	17
B.	GENERAL FORMULATION .....	19
IV.	PROBLEM FORMULATION .....	25
A.	LASER .....	25
B.	TARGET MISSILE .....	31
C.	SIMULATION ENVIRONMENT .....	34
V.	CYLINDRICAL CLOAKING MATERIAL SOLUTION .....	35
A.	SOLUTION SETUP .....	35
B.	COMSOL SIMULATIONS .....	43
VI.	CYLINDRICAL DEFLECTION MATERIAL SOLUTION .....	51
A.	SOLUTION SETUP .....	51
B.	COMSOL SIMULATIONS .....	51
VII.	CONCLUSIONS .....	61
A.	FINDINGS .....	61
B.	MATERIAL SOLUTIONS LIMITATIONS .....	62
	APPENDIX. MODELING AND SIMULATION TUTORIAL FOR COMSOL 4.0 ...	67
	LIST OF REFERENCES .....	77
	INITIAL DISTRIBUTION LIST .....	79

THIS PAGE INTENTIONALLY LEFT BLANK

## LIST OF FIGURES

Figure 1.	FEL basic layout from [1].....	3
Figure 2.	Depiction of the possible future of the FEL in U.S. Naval onboard ship defense from [4].....	5
Figure 3.	Graphical portrayal of a material outer layer redirecting electromagnetic energy away from sensitive components from [6].....	9
Figure 4.	In conventional materials $\epsilon, \mu$ derive from the constituent atoms; in metamaterials $\epsilon_{eff}, \mu_{eff}$ derive from sub-units which are macroscopic systems whose size are of the order of the wavelength of light of interest from [7].....	11
Figure 5.	The difference in the optical density of air and 'normal' water (left) causes a straw in a glass of water to seem to be shifted at the interface and slightly enlarged inside the liquid. In 'negative-index water' (right), the straw would seem to continue in 'the wrong direction' from [8].....	14
Figure 6.	Various polygonal and elliptical invisibility cloaks from [9].....	18
Figure 7.	Simple cubic lattice of points in co-coordinate system (left) maps into a distorted mesh in the other co-coordinate system (right) from [11]....	20
Figure 8.	Left: in the $x, y, z$ coordinate system, space is single valued and a ray progresses through the region of negative refraction. Right: an equally legitimate view point is that the refractive index is everywhere positive, but space is triple valued, doubling back on itself so that each point within range of the lens is crossed three times from [7].....	22
Figure 9.	Laser impact and the vaporization jet formed from [13].....	27
Figure 10.	Snapshot of the electric field distribution around the beam waist of a Gaussian beam. In this example, the beam radius is only slightly larger than the wavelength, and the beam divergence is strong. The field pattern is moving from left to right (i.e., toward larger $x$ ) from [15]. ....	29
Figure 11.	(A) Intensity and electric field amplitude of a Gaussian laser beam from [16]. (B) Image shows	

	the Gaussian laser light intensity of a TEM00 dominant mode from [16].....	30
Figure 12.	A Boeing Harpoon AShM from [18].....	32
Figure 13.	The thick blue line shows the path of the same ray in (A) the original Cartesian space, and under two different interpretations of the electromagnetic equations, (B) the topological interpretation and (C) the materials interpretation. The position vector $\vec{x}$ is shown in both the original and transformed spaces, and the length of the vector where the transformed components are interpreted as Cartesian components as shown in (C) from [10]..	36
Figure 14.	Rays traversing a cylindrical cloak at an oblique angle. The transformation media that comprises the cloak lies in an annular region between the cylinders from [10].....	41
Figure 15.	Shows the incident electric Gaussian beam which is used in the simulations.....	44
Figure 16.	Z-component of the resulting electric field for the 2D cloaked cylindrical shell.....	45
Figure 17.	Electric field magnitude for the 2D cloaked cylindrical shell.....	45
Figure 18.	Shifted 0.05 cm. Z-component of the electric field for the 2D cloaked cylindrical shell.....	47
Figure 19.	Shifted 0.05 cm. Electric field magnitude for the 2D cloaked cylindrical shell.....	47
Figure 20.	Shifted 0.1 cm. Z-component of the electric field for the 2D cloaked cylindrical shell.....	48
Figure 21.	Shifted 0.1 cm. Electric field magnitude for the 2D cloaked cylindrical shell.....	48
Figure 22.	Shifted 0.15 cm. Z-component of the electric field for the 2D cloaked cylindrical shell.....	49
Figure 23.	Shifted 0.15 cm. Electric field magnitude for the 2D cloaked cylindrical shell.....	49
Figure 24.	Shows the incident electric plane wave that is used in the simulations.....	52
Figure 25.	$\epsilon=\mu=3$ . Z-component of the resulting electric field for the 2D cylindrical shell.....	53
Figure 26.	$\epsilon=\mu=2$ . Z-component of the resulting electric field for the 2D cylindrical shell.....	54
Figure 27.	$\epsilon=\mu=1$ . Z-component of the resulting electric field for the 2D cylindrical shell.....	54
Figure 28.	$\epsilon=\mu=0.5$ . Z-component of the resulting electric field for the 2D cylindrical shell.....	55

Figure 29.	$\epsilon = \mu = 0.1$ . Z-component of the resulting electric field for the 2D cylindrical shell.....	55
Figure 30.	$\epsilon = \mu = 0.01$ . Z-component of the resulting electric field for the 2D cylindrical shell.....	56
Figure 31.	Shows the incident Gaussian beam that is used in the deflection material solution simulations.....	57
Figure 32.	$\epsilon = \mu = 0.01$ . Resulting electric field magnitude for the 2D cylindrical shell.....	58
Figure 33.	$\epsilon = \mu = 0.01$ . Shifted 0.05 cm. Resulting electric field magnitude for the 2D cylindrical shell....	59
Figure 34.	$\epsilon = \mu = 0.01$ . Shifted 0.1 cm. Resulting electric field magnitude for the 2D cylindrical shell....	59
Figure 35.	$\epsilon = \mu = 0.01$ . Shifted 0.15 cm. Resulting electric field magnitude for the 2D cylindrical shell....	60

THIS PAGE INTENTIONALLY LEFT BLANK

## LIST OF TABLES

Table 1.	Boeing AGM-84 Harpoon AShM Specifications [17]..	32
Table 2.	AShM Modeling and Simulation Specifications.....	33

THIS PAGE INTENTIONALLY LEFT BLANK



## LIST OF ACRONYMS AND ABBREVIATIONS

AShM	Anti-Ship Missile
C-DEW	Counter-Directed Energy Weapons
CG	Guided Missile Cruiser
DEW	Directed Energy Weapons
DDG	Guided Missile Destroyer
FEL	Free Electron Laser
FFG	Guided Missile Frigate
LHA	Amphibious Assault Ship
LHD	Amphibious Helicopter Assault Carrier Dock
LPD	Amphibious Transport Dock
LSD	Landing Ship Dock
MLD	Maritime Laser Demonstration
NRL	Naval Research Laboratory
ONR	Office of Naval Research

THIS PAGE INTENTIONALLY LEFT BLANK

## **I. INTRODUCTION**

The subject matter pertaining to the problem statement takes into account a wide variety of topics. A concise and brief introduction to the background subjects of this thesis are provided as a resource to the reader.

### **A. DIRECTED ENERGY WEAPONS (DEW)**

A directed energy weapon is a weapon system that uses targeted energy instead of a projectile. The weapon system transfers energy from the source to the target, for the desired effect. The energy can come in various forms, such as electromagnetic radiation (typically lasers), accelerated particles with mass (particle beam weapons), sound (sonic weaponry), and fire (flamethrowers).

These weapons have often been seen in science fiction and movies, but they are becoming a reality, and much research is being done in this area in the form of basic and applied physics. The Navy is specifically interested in the areas of high-powered lasers or high-powered microwaves as eventual weapons, and these areas of research have been under investigation since the 1960s.

### **B. FREE ELECTRON LASER (FEL)**

The DEW system that pertains most to the thesis problem statement of defending against an electromagnetic beam weapon is the FEL. The following provides an introduction to the specifics of the system.

## 1. Background

A FEL system yields the same optical properties as a conventional laser (most importantly, coherent electromagnetic radiation which can reach high power), however, beam formation takes place using very different operating principles. Gas, liquid, and solid-state lasers use electrons in bound atomic or molecular states to create the beam after the electrons are excited. A FEL uses a relativistic electron beam that is freely flowing, which has very different physics behind beam formation.

In a FEL, a beam of electrons is accelerated to very high speeds (close to the speed of light). The electron beam passes through a FEL undulator or "wiggler" section. The undulator is composed of magnets with alternating poles along the laser cavity. The undulator forces the electrons to follow a sinusoidal path. A product of the electron's acceleration within the undulator is the release of photons (light). Now, the significant attribute of the sinusoidal motion of the electrons is that they are forced into phase with the field, and so that the light being released will also be in phase with the field. The important result is that the emitted light, in phase with the field, will be coherently added together. Through the use of mirrors, the electromagnetic radiation can be stored within the laser cavity. A basic layout of a typical FEL is displayed in Figure 1.

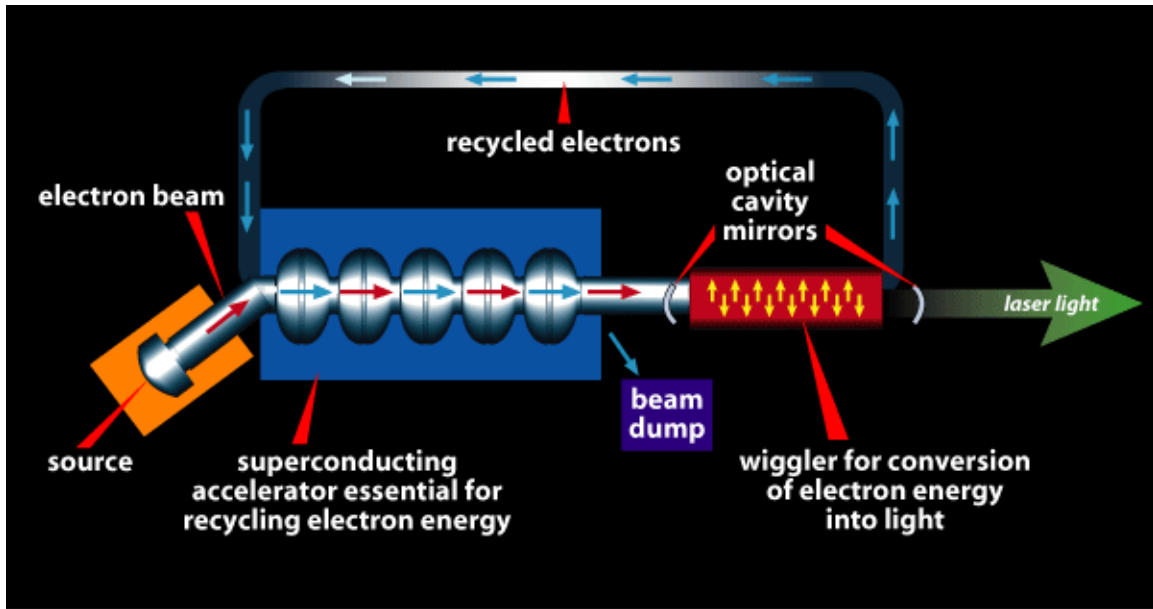


Figure 1. FEL basic layout from [1].

## 2. Navy FEL Relevance

The Office of Naval Research (ONR) has specific interests in this area of physics, based on its possible application to the Navy's future in fighting warfare. The ONR started development and implementation of the Maritime Laser Demonstration (MLD) Program to achieve the goal of creating an eventual shipboard DEW system. The MSD Program will develop a DEW laser based "proof-of-concept" technology. The program is scheduled to create and demonstrate a finished and working tactical system by the end of the decade, which will meet the survivability and self-defense requirements laid out by the U.S. Navy, in response to defeating a variety of small surface boat threats. The MLD Program and DEW system will support, at a very minimum, the DDG, CG, LSD, LPD, LHA, LHD, and FFG ship

classes. The goal of the program is to develop and test a system, which will lead to a subsequent U.S. Naval maritime laser-based weapon System [2].

The U.S. Navy has interest in the development of a FEL because it may be utilized to provide U.S. Naval platforms with a highly effective and affordable point defense capability. The Navy believes that this technology will be a revolutionary gain, transforming ship defense. It is envisioned to be used tactically to defeat various surface and air threats, future anti-ship missiles (AShM), and swarms of small boats. In addition, other possible missions include "soft kills," as well as extending the mission to shore with relay mirrors to cut tank treads, melt gun barrels, cut cables and communications, etc. The Navy also sees other benefits to an onboard FEL system, which includes use of this technology to provide counter-surveillance at sea, advanced maritime situational awareness, and high-resolution imagery with a beam director. The development of a FEL onboard weapon system has been deemed a "game changer" for the U.S. Naval warfare mission [3]. A pictorial realization of this technology is depicted in Figure 2.



Figure 2. Depiction of the possible future of the FEL in U.S. Naval onboard ship defense from [4].

Unlike today's conventional onboard defense, the new FEL weapon system would allow an unlimited supply of ammunition, with speed-of-light delivery. Speed-of-light delivery will eliminate the maneuver advantage of the target. Current defenses feature projectile-based weapon systems, such as missiles and Phalanx guns. It has been recognized for some time that our adversaries have been researching and developing technologies that could penetrate our current missile and gun-based defenses. New missiles under development can fly at lower altitudes and higher speeds, with ever-increasing maneuverability and reduced detection signatures. For every evasive  $g$  [gravity force] a

combatant threat can maneuver, a defensive weapon system must incorporate three additional g's for required kill probabilities [4]. It is viewed that current defense technology could be reaching physical limits, as well as financial constraints, in keeping up with new attack technologies [4].

A FEL weapon system would advantageously allow high depth-of-fire, with only seconds of dwell time. It would be used for a wide range of missions and threats, by being designed to have both selectable wavelengths, as well as the ability to control the strength of the beam for graduated lethality or specific missions. It would allow precise engagement with little collateral damage, compared to explosive munitions. The FEL will, in theory, be powerful, efficient, and reliable. Current FEL systems can run 24 hours a day, for weeks at a time. The FEL system, also, in a purely economical sense, will save money. It would be an alternative to the use of expensive ordinance against the mission compatible targets. An engagement lasting just a few seconds, would burn only a few gallons of fuel, costing the Navy very little for an effective weapon, compared to current conventional expensive weapons. Operational cost is important for any weapon system. The lifetime cost of a FEL weapon system could be a huge savings to a Navy budget [3].

Thus, the FEL seems to be the future for the U.S. Navy defense. However, currently, it is still in the basic stages of development. At this time, an Innovative Naval Prototype (INP) program is underway, with the goal of creating a scalable prototype of an eventual megawatt-class device. The program's focus will be on the design, development,



fabrication, integration, and testing of a 100-kW class FEL weapon system [3]. Current research is stepping away from the entire FEL system background. The focus is directed towards pushing the individual subcomponents and subsystems to their limits to get the power requirements to the needed specifications [4].

## **C. COUNTER-DIRECTED ENERGY WEAPONS (C-DEW)**

### **1. Navy Relevance**

As part of an initiative for future survivability and self-defense of the U.S. fleet, ONR, in conjunction with the Naval Postgraduate School, U.S. Naval Academy, and the Naval Research Laboratory have begun investigating basic research into the area of countering DEW system threats [5].

The introduction chapter thus far has attempted to make a case for DEW systems as the future of warfare for the U.S. Navy. However, these advances in DEW systems will not be one-sided and, as a result, C-DEW interest is becoming a topic of great interest. The ONR C-DEW program is investigating and developing basic research that will focus on providing operational effectiveness in defending against various known and projected airborne, surface, ground, and underwater DEW systems threats. Basic research studies will be conducted on new technologies, techniques, tactics, and procedures for combating DEW threats [5].

### **2. Problem Description**

C-DEW is a large topic and very diverse in its research. The focus of this thesis is to explore the physics of redirecting, deflecting, and/or reflecting energy from an

electromagnetic weapon, such as a FEL, described earlier in this introduction. The FEL is likely to be one of the threats of the future, and one of the proposed defenses against such a threat involves a material sided solution in the form of a protective outer layer.

Various material based solutions and techniques of application have been proposed for electromagnetic beam defense. The material solution of interest to this thesis topic is a solution that would entail a highly engineered material, which would act as a defensive outer layer. This material would either deflect the light energy, or direct it through the material around any mission critical components. A graphical portrayal of such a defense is shown in Figure 3.

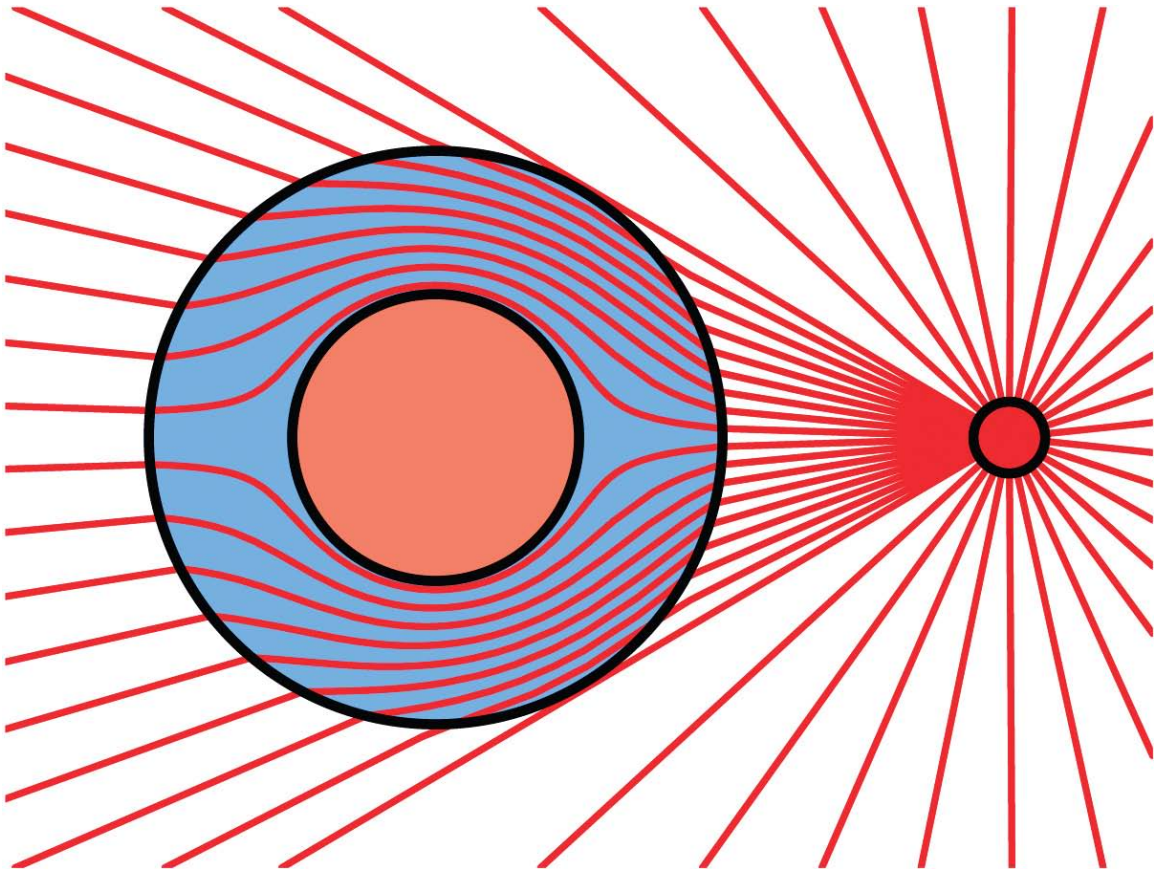


Figure 3. Graphical portrayal of a material outer layer redirecting electromagnetic energy away from sensitive components from [6].

It has been proposed through the use of metamaterials and transformational optics (both of which will be discussed in detail in subsequent chapters) that perhaps a material could be engineered and manufactured that would have the intrinsic properties to redirect and/or deflect radiation, as a primary form of defense against an electromagnetic energy threat.

The goal of writing this paper is to research such materials, learn and understand the physics of transformational optics, apply the material and physics to the problem of electromagnetic defense, explore computer

modeling and simulation of the problem, address the future applicability of such a solution, and, finally, to determine whether future research in this area may be justified.

## II. METAMATERIALS

### A. BACKGROUND

Metamaterials are a new class of materials that possess intrinsic electromagnetic properties that do not normally exist in nature. As a result, they are highly engineered and often require a very complex manufacturing process. Their abnormal intrinsic electromagnetic properties are due to their sub-wavelength structure, which is obviously significantly different than most materials whose intrinsic properties rely on their inherent chemical composition [6]. A depiction of the underlying structural differences is presented in Figure 4.

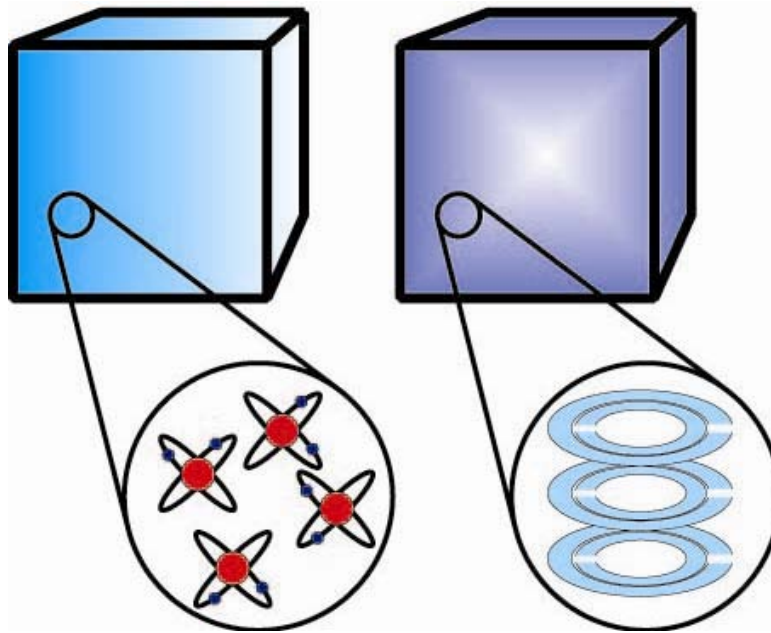


Figure 4. In conventional materials  $\epsilon, \mu$  derive from the constituent atoms; in metamaterials  $\epsilon_{eff}, \mu_{eff}$  derive from sub-units which are macroscopic systems whose size are of the order of the wavelength of light of interest from [7].

Conventional materials interact with light according to the individual atoms and molecules from which they are made [7]. Of main interest to physicists are the macroscopic electromagnetic fields, which interact with the material. These macroscopic fields are nothing more than averages over the fluctuating local fields. However, these macroscopic fields are very well determined because there are typically billions of molecules per cubic wavelength of matter [7]. Metamaterials mimic the building block structure of nature, by replacing the molecules by man-made structures. To construct materials with the effective properties for a specific wavelength, the underlying structures must have characteristic lengths smaller than that of the wavelength for which they have been designed. For example, the metamaterial underlying structure might have dimensions of nanometers for visible light, or up to a few millimeters for microwave radiation [7].

The highly significant excitement relating to metamaterials lies in the fact that their inherent inhomogeneous design offers a completely novel approach to controlling light. It is now thought that the future of metamaterials will be a manufacturing process, in which a structure will be designed on the sub-wavelength scale, in which its permittivity and permeability values will be designed to be independently determined within the structure [6]. The resulting structure would have a varying index of refraction tailored according to its specific electromagnetic design requirements. Conceivably, one could design and manufacture materials whose refractive index could virtually guide light through any path within the material. As a result, metamaterial applications are

abundantly being theorized and designed. The problem, however, lies not in the application, but the availability of methods to engineer and manufacture the appropriate metamaterials. It is very apparent that the theory and formulation behind controlling light within a material is far beyond the current technology and ability to manufacture these complex materials. However, the development of new and more complex manufacturing techniques is increasing at an astonishing rate. As a result, research into a metamaterial solution to the problem of redirecting and deflecting of an electromagnetic energy source should not be hindered by the current technology available for manufacturing. Current basic research must be done to determine if such solutions are viable and can be computer-simulated, while manufacturing technologies catch up with theoretical goals.

## **B. PROPERTIES**

Metamaterial structures, as described earlier, are engineered and have properties not associated with materials normally found in nature. An almost unsettling depiction into the unnaturalness of the properties of light interaction within metamaterials is rendered in Figure 5, which shows what a fictional metamaterial could do.

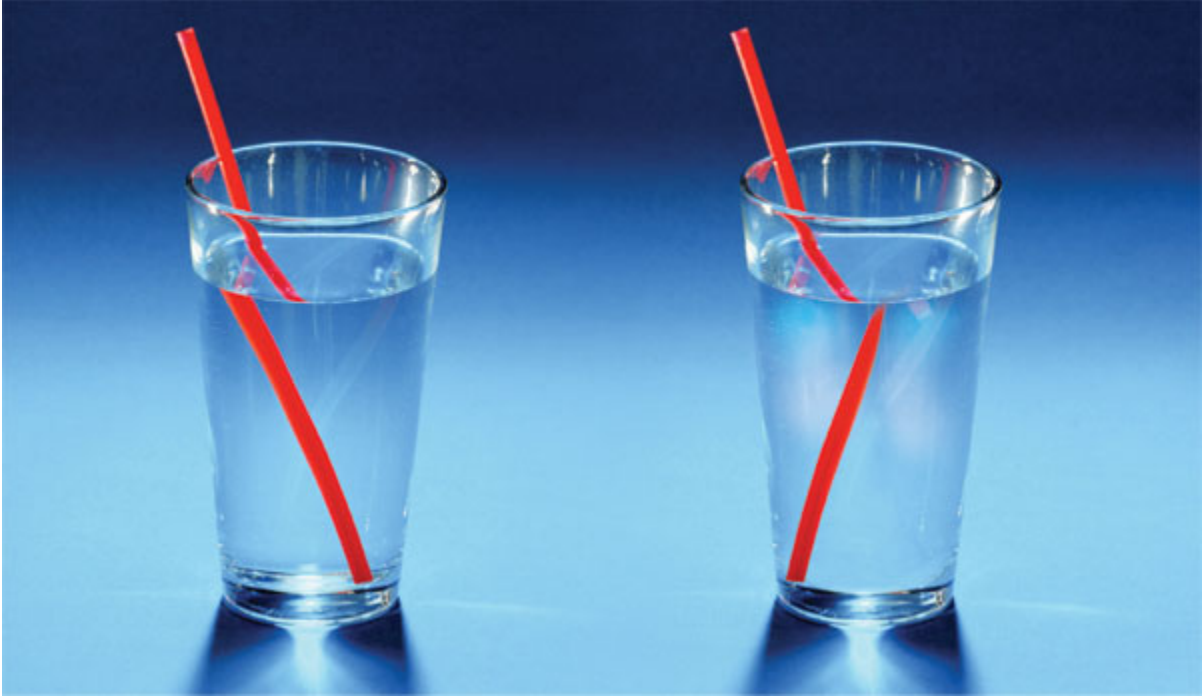


Figure 5. The difference in the optical density of air and 'normal' water (left) causes a straw in a glass of water to seem to be shifted at the interface and slightly enlarged inside the liquid. In 'negative-index water' (right), the straw would seem to continue in 'the wrong direction' from [8].

A metamaterial affects incident electromagnetic radiation if its underlying structure is smaller than the wavelength of the incident radiation. As a result, the smaller the wavelength, the more complex the material's manufacturing process will be. This fact is an important and differentiating plus for material solutions in electromagnetic radiation defense. A FEL beam, to be of any use, must travel through the atmosphere over a certain range to its target. In the design and application process for a FEL, smaller and smaller wavelengths of radiation are instantly ruled out, due to interaction with the atmosphere



itself. It is predicted that a FEL laser being used as a weapon will generally operate in the infrared to microwave wavelength range. This implies, for C-DEW defense, a metamaterial structure that may be easier, albeit not currently possible to manufacture.

An important and fundamental aspect of engineering metamaterials is loss. Currently, known metamaterials are generally comprised of metallic materials that will undesirably absorb a great deal of the incident radiation. This poses a concern because if the material is damaged while redirecting a high-powered laser beam (due to overheating, melting, or disintegration) then the material could become less effective. As a result, a metamaterial solution layer would have to be highly efficient considering the power magnitudes proposed by FEL weapon systems currently being developed. While the problem of loss is a current drawback, it is also an inevitable constraint on a material sided solution. However, it does not justify abandoning the basic nature of research in this thesis.

Considerable research is currently being undertaken to design more efficient metamaterial structures. One advantage in this line of research is that metamaterials have so many desired applications. The application abundance is translating into a lot of positive hype. As a result there is a growing industry investing in the science of engineering and manufacturing of new and more efficient metamaterials.

### **C. DESIGN AND MANUFACTURING**

At frequencies in the GHz range, conversion of energy to heat loss in currently designed metamaterials is mainly attributed to the dielectric component of the structure of the material [7]. Loss in this range becomes less of an issue when compared to metamaterials designed for higher frequency regimes [7]. Also, frequencies in this range translate to longer wavelength scales. This requires the manufacture of less complex micro-structures that is within reach of current technology [7]. Perhaps the most limiting aspect of research into metamaterials is the need for cheap and efficient manufacturing techniques capable of making these 3D structures [7]. Most designs are assembled by building up 2D panels on top of one another, in a very low tech way. This process will have to be improved and optimized before metamaterial promise and designs can be utilized outside of the laboratory [7].

### III. TRANSFORMATIONAL OPTICS

#### A. BACKGROUND

In optical physics, every material can be defined by its refractive index property. It is defined to be the ratio between the speed of the electromagnetic radiation passing through a vacuum ( $c$ ) and the speed of the wave propagating through the material ( $v_p$ ) for a given wavelength:

$$n = \frac{c}{v_p} \quad (3.1)$$

In terms of electromagnetic radiation, the index of refraction is comprised of the material properties of permittivity ( $\epsilon$ ), the polarizability response due to an electric field, and the permeability ( $\mu$ ), the response due to a magnetic field.

$$n = \sqrt{\epsilon \cdot \mu} \quad (3.2)$$

Most materials have refractive indices larger than one. One can see from the above equation that a negative index of refraction is impossible to achieve. However, over the last decade, significant research has been done to use common materials with indexes above one and arranging them in ways that their structure rather than their individual indices determine the composite's electromagnetic properties. Metamaterials are examples of this concept that allow, in theory, composite structures with negative indices of refractions.

Variability of a material's refractive index is the basis for construction of metamaterials that have the property of being able to guide electromagnetic radiation as it propagates within the material. Transformational optics is a fairly recent branch of mathematical physics that theoretically postulates ideas that have traditionally been exclusive to science fiction. Research is currently being done in the areas of cloaking, invisibility, electromagnetic wormholes, and perfect lenses (resolution beyond the limits of wavelength). A few pictures of invisibility cloaks are shown in Figure 6.

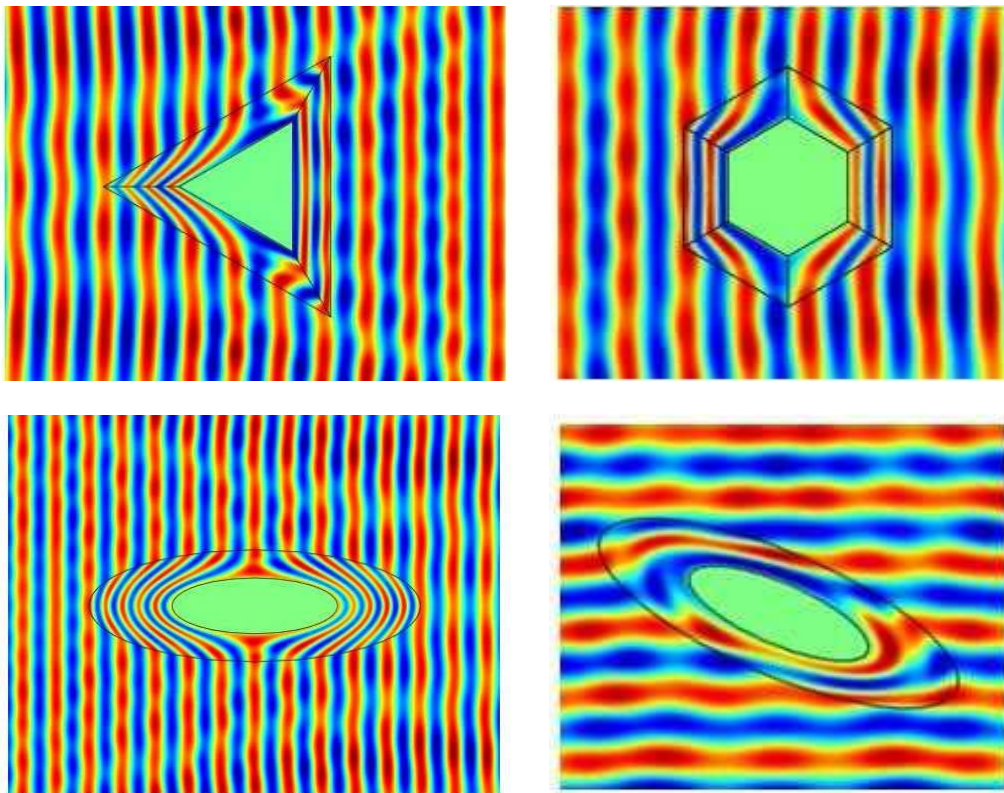


Figure 6. Various polygonal and elliptical invisibility cloaks from [9].

The rise of transformational optics, and the interest in metamaterials, invites the possibility of a material solution as a counter to the threat of a high-energy electromagnetic radiation weapon. Utilizing a material layer, it is hypothesized that it could cloak or simply divert the incident radiation around or away from high value or sensitive components. Both possibilities will be explored in this thesis. However, we first must give a general formulation of transformational objects, so that we may have a more complete understanding of the development of each.

## B. GENERAL FORMULATION

The method of transformational optics for Maxwell's equations is outlined by J.B. Pendry, D. Schurig, and D.R. Smith in [10]. The method uses Cartesian tensors to create a blueprint for the required material properties of the metamaterials. This paper uses the Minkowski form of Maxwell's equations for a general space-time transformation from which results of [10] are reported below. A complete derivation of the equations is unnecessary and beyond the necessary scope of this thesis. Equations presented are used to set up a possible material solution to the problem in Chapter IV.

Maxwell's equations governing propagation of electric and magnetic fields through space without sources or currents in Cartesian coordinates are:

$$\begin{aligned}\nabla \times \vec{\mathbf{E}} &= -\mu\mu_0 \frac{\partial \vec{\mathbf{H}}}{\partial t}, \\ \nabla \times \vec{\mathbf{H}} &= \varepsilon\varepsilon_0 \frac{\partial \vec{\mathbf{E}}}{\partial t}\end{aligned}\tag{3.3}$$

In this form, the permittivity ( $\varepsilon$ ) and the permeability ( $\mu$ ) are generally tensors. The form of the equations gives the freedom that both  $\varepsilon$  and  $\mu$  may depend on the position within space. Next, we wish to transform the Cartesian system to that of a new coordinate system defined by,

$$x'_1(x_1, x_2, x_3), x'_2(x_1, x_2, x_3), x'_3(x_1, x_2, x_3) \quad (3.4)$$

Because these are completely generalized, coordinates equally spaced points along the  $x'_1, x'_2, x'_3$  axes may appear distorted in the original  $x_1, x_2, x_3$  coordinate frame. See Figure 7.

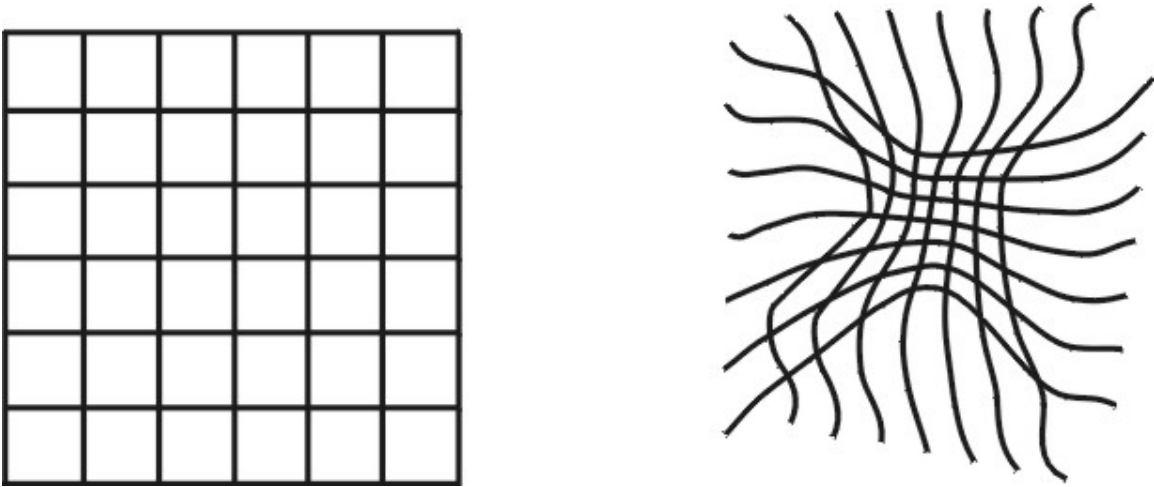


Figure 7. Simple cubic lattice of points in co-coordinate system (left) maps into a distorted mesh in the other co-coordinate system (right) from [11].

Thus far, Maxwell's equations have been written in the original Cartesian system. Expressed in terms of the new coordinates -  $x'_1, x'_2, x'_3$ , the transformed set of equations in the primed coordinate system becomes

$$\begin{aligned}\nabla' \times \bar{\mathbf{E}}' &= -\mu' \mu_0 \frac{\partial \bar{\mathbf{H}}'}{\partial t}, \\ \nabla' \times \bar{\mathbf{H}}' &= \varepsilon' \varepsilon_0 \frac{\partial \bar{\mathbf{E}}'}{\partial t}\end{aligned}\tag{3.5}$$

where  $\varepsilon'$  and  $\mu'$  are again tensors, and  $\bar{\mathbf{E}}'$  and  $\bar{\mathbf{H}}'$  are renormalized electric and magnetic fields. The takeaway from this transformation is that all four new quantities are related to their originals. This is important because it means that Maxwell's equations are preserved through the transformation.

According to the coordinate transformation method, under a space transformation from a flat space  $x$  to a distorted one  $x'(x)$ , the tensors of permittivity  $\varepsilon'$  and permeability  $\mu'$  for a linear, anisotropic, non-dispersive, non-bianisotropic medium in the transformed space can be written as [12]:

$$\begin{aligned}\bar{\mathbf{E}}' &= (\mathbf{A}^T)^{-1} \bar{\mathbf{E}}, \quad \bar{\mathbf{H}}' = (\mathbf{A}^T)^{-1} \bar{\mathbf{H}} \\ \mu' &= \frac{1}{\det \mathbf{A}} \mathbf{A} \mu \mathbf{A}^T, \quad \varepsilon' = \frac{1}{\det \mathbf{A}} \mathbf{A} \varepsilon \mathbf{A}^T\end{aligned}\tag{3.6}$$

where the matrix  $\mathbf{A}$  is the Jacobian transformation matrix that is defined by

$$A_{ij} = \frac{\partial x'_i}{\partial x_j}, \quad A_{ij}^{-1} = \frac{\partial x_i}{\partial x'_j}\tag{3.7}$$

These equations represent the exact transformations from one orthogonal coordinate system to another for the Maxwell equations. They define the building blocks  $(\varepsilon, \mu)$  that enable that transformation to be possible. The vital point is that these equations give a way to move fields within matter,

based on design. The birth of metamaterials has given rise to, and the ultimate promise of, being able to ultimately control electromagnetic waves through matter. We will use Equations (3.6) and (3.7) in Chapter V to form and develop a possible material solution to the problem of directing electromagnetic waves to protect from a DEW threat.

First, however, as an example outlined by [7], we apply transformational optics and Equations (3.6) and (3.7) to gain insight into another interpretation of the Veselago lens, which is depicted in Figure 8.

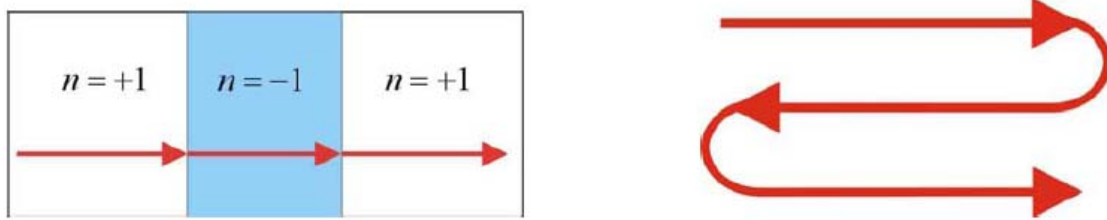


Figure 8. Left: in the  $x,y,z$  coordinate system, space is single valued and a ray progresses through the region of negative refraction. Right: an equally legitimate view point is that the refractive index is everywhere positive, but space is triple valued, doubling back on itself so that each point within range of the lens is crossed three times from [7].

The Veselago lens exists in real space  $(x,y,z)$ , which is depicted in the image on the left in Figure 8. However, when observing the lens from the outside, one perceives the region between the object plane and the image plane to vanish. The following coordinate transformation expresses this by mapping real space  $(x,y,z)$  on to a triple valued space  $(x',y',z')$ ,



$$\begin{aligned}
y' &= y, \quad z' = z, \\
x' &= x, \quad x < x_1, \\
x' &= (2x_1 - x), \quad x_1 < x < x_1 + d, \\
x' &= x - 2d, \quad x_1 + d < x
\end{aligned} \tag{3.8}$$

where the lens lies in the interval  $x_1 < x < x_1 + d$ . Straightforwardly applying Equations (3.6) and (3.7) to the transformation formulae listed in Equation (3.8) yields,

$$\begin{aligned}
\varepsilon &= \mu = +1, \quad x < x_1, \\
\varepsilon &= \mu = -1, \quad x_1 < x < x_1 + d, \\
\varepsilon &= \mu = +1, \quad x_1 + d < x
\end{aligned} \tag{3.9}$$

This shows that the triple valued distorted space defined by Equation (3.8) can be created using the blueprint for the material properties shown in Equation (3.9), which is exactly how the Veselago lens is defined in Figure 8. This example gives a geometrical interpretation to the lens. The interpretation is that the Veselago lens is comprised of a section of 'negative' space that annihilates an equivalent thickness of vacuum [7].

THIS PAGE INTENTIONALLY LEFT BLANK

## IV. PROBLEM FORMULATION

High-energy electromagnetic radiation weapons (e.g. a FEL) are the future of U.S. Naval warfare, and are anticipated to, not only be realized in the next decade, but to be operational. It is foreseeable that our opponents will also develop such weapons, and therefore, we must create defenses against such threats. The primary mission being explored is that of close-in carrier missile engagement defense. It is foreseeable that U.S. adversaries will be developing said weapon systems for the same mission.

There are countless uses for metamaterials and transformation optics, some most likely have not even been idealized, as of yet. But for the purpose of this thesis, we will explore two material solutions to the defense of a hostile electromagnetic radiation beam weapon upon a U.S. inbound missile. In order to properly, even if loosely, simulate the laser and the missile, we must first define the parameters, assumptions, approximations, and environment to which our computer simulations will be conducted. The next few sections will define the model, which will be used to best test and explore the possible material solutions that will be analyzed in the follow-on chapters.

### A. LASER

To model an enemy hostile laser, we will need to make some generalities, approximations, and assumptions needed to model both proposed theoretical material solutions. First of all, we will model the entire system to be a steady state simulation. A FEL generally operates tactically on a "dwell

time," where it is predicted that a beam a few seconds on target will destroy up to approximately 1 litre of material. We will take the entire laser beam model to be in a steady state environment, and are interested in how the electromagnetic radiation interacts with the target and how in the presence of the possible material solutions will determine the resulting fields. This is not exactly the case, because the beam will not exactly be incident on the same spot for a few seconds duration. A way to think about the simulation model is an instantaneous snapshot of the incident and resulting electromagnetic fields in the presence of the material solutions.

We will generalize the hostile laser in the simulations as having a wavelength of 5 cm. Electromagnetic radiation weapons are idealized to operate as a weapon in-between the infrared and microwave wavelength regions, as a result of atmospheric effects and optimum conditions, to perform maximum damage. This puts the chosen simulation wavelength in a suitable spot within the proposed wavelength region, however, a smaller wavelength on the order of a micrometer would be a far more realistic input. The simulations, however, are limited by the meshing requirements of the real dimensions used by the modeling program. It has been determined in modeling this specific problem of a missile, having a diameter dimension on the order of a meter, that anything below the chosen wavelength is difficult to simulate and solve. A more realistic study would include a wavelength input of a Navy FEL weapon system currently being developed. A more important aspect of the problem of a proposed FEL wavelength range is that further study will need to be conducted to determine how applicable and

forgiving a material solution would be in regard to variation in frequency, since metamaterials are very specifically designed, based on a specific incident light wavelength. If the laser is assumed to be able to be tuned, this could have a drastic importance of whether the metamaterial solutions presented are even remotely viable.

During a laser impact, a miniscule layer of material is melted and then vaporized. The vaporization of the material forms a vapor jet. The liquid metal is pushed away from the spot location towards the edge [13]. As a result, a proper model must take into account the material thermodynamic properties, the matter ablation, and the molten metal motion [13] as shown in Figure 9.

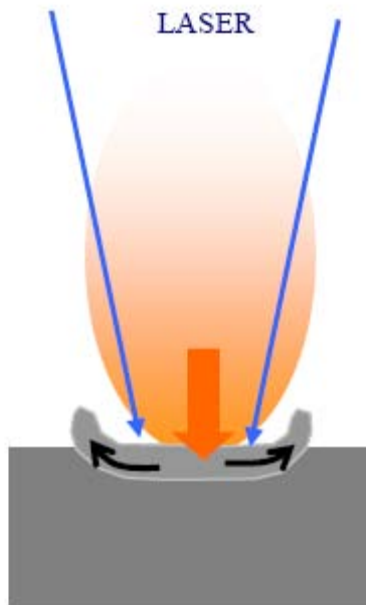


Figure 9. Laser impact and the vaporization jet formed from [13].

However, we will make the approximation that the electromagnetic beam interacts with the material, without

the physical processes that have just been described. We are more interested in the basic research of the fields that arise from interaction with the material solutions than the thermodynamic properties at the boundary layers and the drilling that may or may not occur. Shining a FEL on possible material solutions, presented in this thesis would be an excellent topic for further research, depending on the results determined.

We will model the hostile incident electromagnetic beam as one, which approximates a Gaussian profile. In this case, the beam is said to be operating on the fundamental transverse mode. This is a good approximation because Gaussian beams are often the simplest and most desirable type of beam for a laser source [14]. A laser beam, in reality, is a 3D problem, however we will approximate the beam in all simulations as a 2D laser beam in which there will be one transversal dimension  $x$  and one axial dimension  $r$ . The expression for the complex electric field amplitude distribution of a Gaussian laser beam propagating in the  $x$  direction can be written as in [15],

$$E(r, x) = E_0 \frac{w_0}{w(x)} \exp\left[-\frac{r^2}{w^2(x)}\right] \exp\left[-ikx + i \tan^{-1}\left(\frac{x}{x_R}\right) - \frac{ikr^2}{2R(x)}\right] \quad (4.1)$$

Where  $r$  is the radial distance from the center axis of the beam,  $x$  is the axial distance from the beam's narrowest point (the "waist") and the direction of propagation,  $|E_0|$  is the peak amplitude,  $x_R = \frac{\pi w_0^2}{\lambda}$  is the Rayleigh length, which determines the length over which the beam can propagate

without significantly diverging,  $w(x) = w_0 \sqrt{1 + x/x_R}$  is the beam radius, with  $w_0$  being the radius at the beam waist,  $k = \frac{2\pi}{\lambda}$  is the wave number,  $\lambda$  is the wavelength, and  $R(x) = x \left[ 1 + (x_R/x)^2 \right]$  is the radius of curvature of the wavefronts. A fully developed Gaussian laser beam is depicted in Figure 10, and the spot profile is shown in Figure 11.

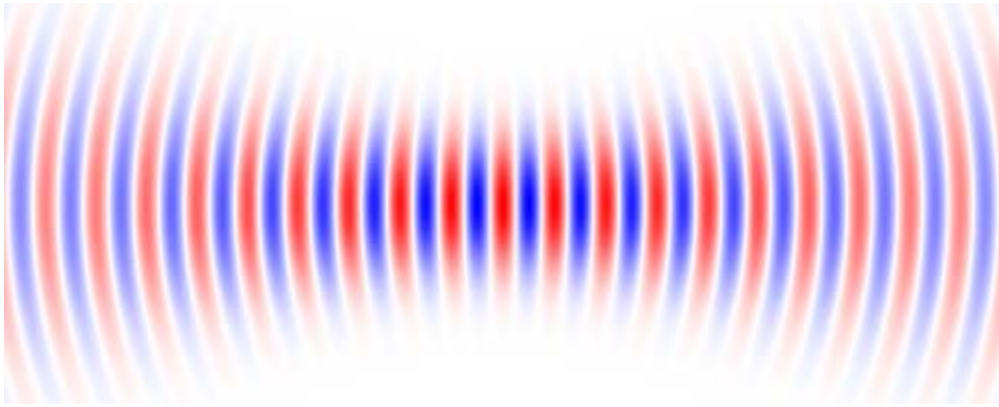


Figure 10. Snapshot of the electric field distribution around the beam waist of a Gaussian beam. In this example, the beam radius is only slightly larger than the wavelength, and the beam divergence is strong. The field pattern is moving from left to right (i.e., toward larger  $x$ ) from [15].

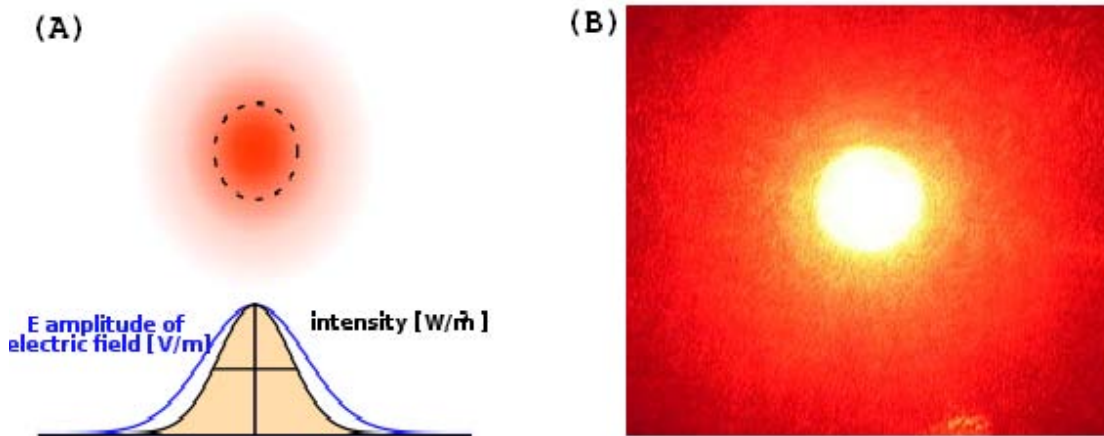


Figure 11. (A) Intensity and electric field amplitude of a Gaussian laser beam from [16]. (B) Image shows the Gaussian laser light intensity of a TEM00 dominant mode from [16].

A subtle yet important aspect of using the 2D complex electric field amplitude distribution of a Gaussian laser beam in our simulations is that it is only an approximation to that of the actual 3D equation. The approximated 2D beam used in simulations does not rigorously satisfy Maxwell's equations. As a result, there will be noticeable effects in the later presented simulations. However, it is felt, that using a 2D approximated laser beam is more beneficial to modeling the problem as a whole than merely using a plane wave in all simulations. All beam simulations will use the approximated 2D Gaussian beam of Equation (4.1) with the following beam properties:

$$\lambda = 5 \text{ cm}$$

$$w_0 = 8 \text{ cm (25\% of the target missile diameter)}$$

$$|E_0| = 1 \text{ (Normalizing the electric field magnitude)}$$



The reasoning behind the chosen input wavelength has already been discussed. The beam waist has been chosen to be 25% of the missile diameter to appropriately model a diverging laser beam that has traveled some distance. Any larger, and the simulation of a plane wave would be justified. Any smaller, and the resulting electric field is difficult to discern visually based on the dimensions of the entire problem. The electric field magnitude has been normalized because the simulations are only concerned with the form of the resulting electric field immediately around and within the material layer.

## **B. TARGET MISSILE**

Based on our setup, we need to define some dimensions about the missile we are going to be modeling and using in the material solution simulations. We will be modeling a very general AShM, and since the purpose of this research topic is a basic research concept (and not to design a specific material solution for a specific U.S. Navy weapon system), we will present numbers as just a general tool and no way should they be construed to be actual future design specifications.

The specifications used in this research were actually found using the "Google" search engine, with the search query being "anti-ship missile dimensions." Given this line of research into possible AShM specifications, a Wikipedia article was discovered that listed all the specifications needed for our modeling and simulation purposes. The Website lists the specifications for the Boeing AGM-84 Harpoon AShM varieties, one of which is reproduced in Table 1.

Table 1. Boeing AGM-84 Harpoon AShM Specifications [17].

<b>Length</b>	<b>Air Launched</b>	<b>3.8 m</b>
	<b>Surface/Submarine Launched</b>	<b>4.6 m</b>
<b>Weight</b>	<b>Air Launched</b>	<b>519 kg</b>
	<b>Surface/Submarine Launched</b>	<b>628 kg</b>
<b>Diameter</b>	<b>0.34 m</b>	
<b>Wing Span</b>	<b>0.914 m</b>	
<b>Speed</b>	<b>240 m/s</b>	
<b>Warhead</b>	<b>221 kg</b>	

In Figure 12, a picture of an AGM-84 Harpoon missile is shown for completeness.



Figure 12. A Boeing Harpoon AShM from [18].

We will make the approximation that the simulated missile is represented by an infinitely long cylinder, and thus simplifies the simulation problem from a 3D problem to a 2D problem. This greatly reduces the complexity of the geometry and inputs, but more importantly reduces the necessary computational processing power to simulate the problem. The 2D cylinder approximation becomes erroneous close to the ends and over non-cylindrical geometries on the rocket (such as fins). However, we will neglect these non-idealized effects in the present analysis of our feasibility study.

We must also make the approximation of a skin layer specification for the proposed missile simulations. The purpose of the missile is to deliver a weapon package to the target, and the goal of the solution is to protect the essential weapon package from an electromagnetic beam threat. The material solution skin layer thickness cannot be unrealistically large in our modeling because that would not be a very effective addition to a current missile system, and would most likely yield any current system ineffective. For the purposes of this thesis, we will model the material solution skin layer as 25% of the overall missile radius. The following dimensions for the modeled target missile, listed in Table 2, will suffice for the remainder of the thesis:

Table 2. AShM Modeling and Simulation Specifications

<b>Package Radius</b>	<b>12 cm</b>
<b>Skin Layer Thickness</b>	<b>4 cm</b>
<b>Missile Radius</b>	<b>16 cm</b>

### **C. SIMULATION ENVIRONMENT**

In analyzing the two possible material solutions presented in this thesis, we have hypothesized parameters for the incident electromagnetic radiation and the missile material solution shell to be modeled. The difference between the two solutions will be in how we design the material properties of the two metamaterial skin layers. In all but the skin layers, the models and simulations will be exactly the same.

To analyze the proposed possible material solutions, we will employ the COMSOL Multiphysics simulation software environment. It allows the user to build, mesh, and solve the entire numerical model in one software environment. We will additionally, and necessarily, use the Radio Frequency (RF) Module, which provides the user the added capability of modeling the propagation of electromagnetic waves in and around the missile structure. Furthermore, the RF Module allows the user to define metamaterials with engineered properties, no matter the anisotropic nature of the material. The finite element-based electromagnetic solver in the COMSOL Multiphysics package is of particular use to this thesis because of the flexibility it allows, in specifying material anisotropy and inhomogeneity within the modeled missile.

To demonstrate the modeling environment, a tutorial for setting up the models using the COMSOL Multiphysics package is presented in the Appendix.

## V. CYLINDRICAL CLOAKING MATERIAL SOLUTION

### A. SOLUTION SETUP

The first possible material solution to our problem of defending against a high-energy electromagnetic threat would be to create a metamaterial shell around sensitive components that could redirect an incident electromagnetic beam around sensitive components. Our solution does not require invisibility as a necessary constraint for defense. Using transformational optics, we derive the geometry and material constraints necessary to design an effective metamaterial cloaking skin.

Using the methodology described by J.B. Pendry, D. Schurig, and D.R. Smith in [10], we have the material constraints required in designing the cylindrical cloak. In essence it is a cylindrically symmetric coordinate transformation that compresses all the space in a volume of radius  $b$  centered about the cylinder into a cylindrical shell of inner radius  $a$  and outer radius  $b$ . To visualize the transformation, consider a position vector  $\vec{x}$  with Cartesian coordinates  $x^i$ . In the transformed space, the position vector will have coordinates  $x^{i'}$  as shown in Figure 13.

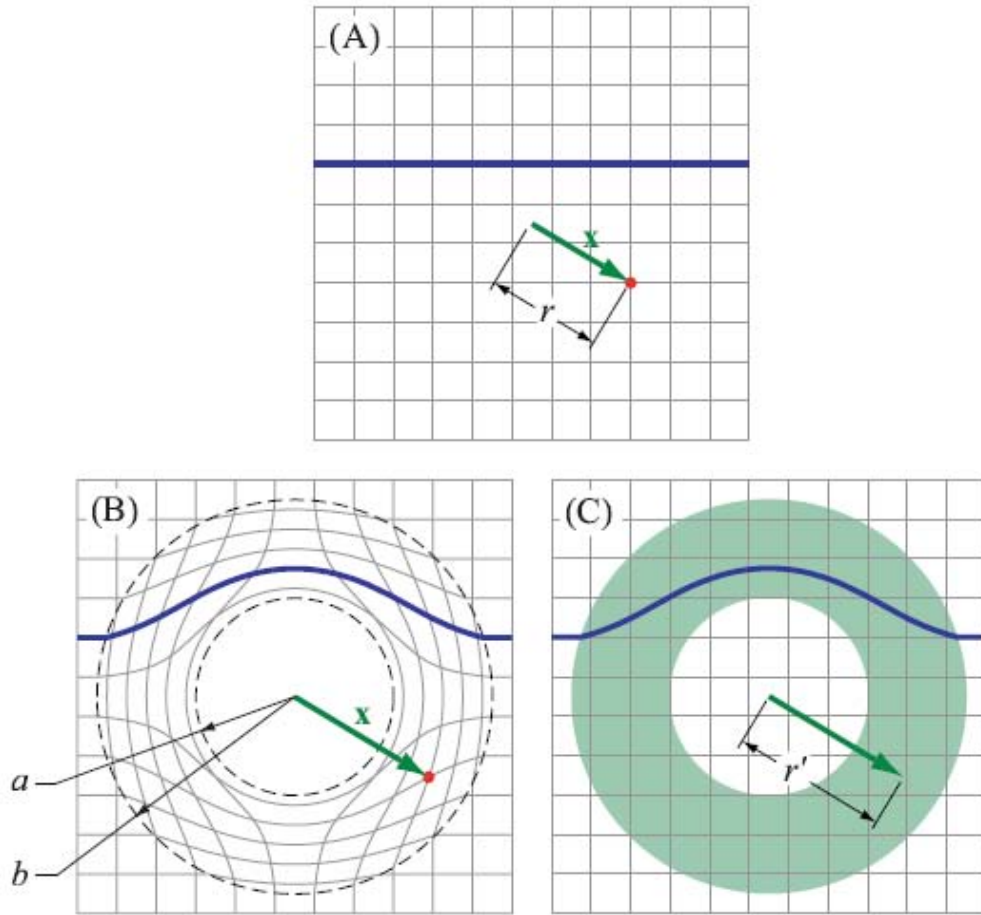


Figure 13. The thick blue line shows the path of the same ray in (A) the original Cartesian space, and under two different interpretations of the electromagnetic equations, (B) the topological interpretation and (C) the materials interpretation. The position vector  $\vec{x}$  is shown in both the original and transformed spaces, and the length of the vector where the transformed components are interpreted as Cartesian components as shown in (C) from [10].

The magnitude,  $r$ , of the vector,  $\vec{x}$ , will of course be independent of the coordinate system and is defined as

$$r = (x^i x^j \delta_{ij})^{1/2} = (x^{i'} x^{j'} g_{i'j'})^{1/2} \quad (5.1)$$

Where  $g_{i'i'}$  is the metric of the transformed space. However, in the materials interpretation we will take the components  $x^{i'}$  to be the components of a Cartesian vector. Also, the magnitude, which we will call  $r'$ , is calculated in Cartesian space by,

$$r' = (x^{i'} x^{j'} \delta_{i'j'})^{1/2} \quad (5.2)$$

The spaces will represent a transformation from a cylindrical space to a cylindrical transformation space. An appropriate transformation for this purpose would be one in which the transformation maps points from a radius  $r$  to a radius  $r'$  as follows,

$$r' = \frac{b-a}{b} r + a \quad (5.3)$$

We see that, importantly, when  $r=0$ , then  $r'=a$ , and that, when  $r=b$ , then  $r'=b$ . We will apply the transformation over the domain,  $0 \leq r \leq b$  (or equivalently,  $a \leq r' \leq b$ ). Outside of the domain, we assume the identity transformation,  $r=r'$ .

Next, we need to relate all the variables together. Since our transformation is radially symmetric, the unit vectors in both the material interpretation and original space are equivalent.

$$\frac{x^{i'}}{r'} = \frac{x^i}{r} \delta_i^{i'} \quad (5.4)$$

Using equations (5.3) and (5.4), we can express the components of the position vector in the transformed space, in terms of only the components in the original space, to obtain,

$$x^{i'} = \frac{b-a}{b} x^i \delta_i^{i'} + a \frac{x^i}{r} \delta_i^{i'} \quad (5.5)$$

Now that we have the relation, we can calculate the transformation matrix  $A_j^{i'}$ .

$$A_j^{i'} = \frac{\partial x^{i'}}{\partial x_j} = \frac{r'}{r} \delta_j^{i'} - \frac{a}{r^3} \delta_j^{i'} x^i x^k \delta_{kj} \delta_i^{i'} \quad (5.6)$$

However, this is not totally correct for our problem. Thus far, we have defined the transformation in a spherical sense. The transformation is the same as that of the spherical case, only that now it is applied only to the two dimensions normal to the cylinder's axis. To analyze a cylindrical transformation, we need the help of two projection vectors: one that projects on to the cylinder's axis, and one that projects onto the plane normal to the cylinder's axis.

$$\begin{aligned} Z_{ij} &= \delta_3^i \delta_3^j \\ T_{ij} &= \delta_1^i \delta_1^j + \delta_2^i \delta_2^j \end{aligned} \quad (5.7)$$

We see that the transformation matrices for spherical and cylindrical geometries will be very similar. The transformation will be the same in the plane, normal to the cylinder's axis, and the transformation in the direction of



the axis of the cylinder will be the identity matrix. We can now rewrite the spherical transformation matrix Equation (5.6) with the help of (5.7) as follows,

$$A_j^{i'} = \frac{r'}{r} T_j^{i'} - \frac{a}{r^3} r^i r^k \delta_{kj} \delta_i^{i'} + Z_j^{i'} \quad (5.8)$$

The transformation matrix can be written out using its components, where  $r$  is now the distance from the cylinder's axis,

$$A_j^{i'} = \begin{pmatrix} \frac{r'}{r} - \frac{ax^2}{r^3} & -\frac{axy}{r^3} & 0 \\ -\frac{axy}{r^3} & \frac{r'}{r} - \frac{ay^2}{r^3} & 0 \\ 0 & 0 & 1 \end{pmatrix} \quad (5.9)$$

As seen in the matrix above, we have now defined the plane, normal to the cylinder's axis as the x-y plane, and the cylinder's axis as the z plane for convenience.

We can easily calculate the determinant that will be needed to determine the material properties by rotating the matrix into a coordinate system where the off-diagonals vanish. We then find the determinant to be,

$$\det(A_j^{i'}) = \frac{r' - a}{r} \frac{r'}{r} \quad (5.10)$$

Now, putting all the pieces together, we are able to solve for the material properties needed to cloak the cylinder. Using Equation (3.7), (5.9), and (5.10) and considering that our original space has both a permittivity

and permeability equal to one, the formula for the material properties in the transformed space in direct notation and dropping the primes are,

$$\boldsymbol{\varepsilon} = \boldsymbol{\mu} = \frac{r}{r-a} \mathbf{T} - \frac{2ar-a^2}{r^3(r-a)} \bar{\mathbf{r}} \otimes \bar{\mathbf{r}} + \left( \frac{b}{b-a} \right)^2 \frac{r-a}{r} \mathbf{Z} \quad (5.11)$$

Finally, if we rotate the system to where the off-diagonal elements vanish, we get the individual components of the material parameters for a cylinder in cylindrical coordinates.

$$\varepsilon_r = \mu_r = \frac{r-a}{r} \quad (5.12)$$

$$\varepsilon_\phi = \mu_\phi = \frac{r}{r-a} \quad (5.13)$$

$$\varepsilon_z = \mu_z = \left( \frac{b}{b-a} \right)^2 \frac{r-a}{r} \quad (5.14)$$

A visual depiction of the cloak designed is presented in Figure 14.

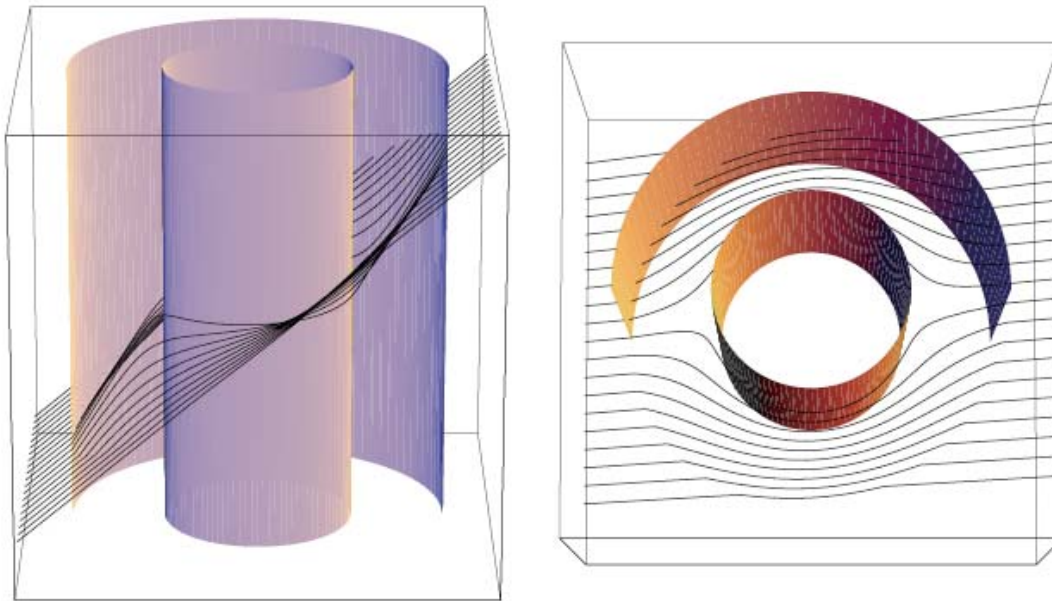


Figure 14. Rays traversing a cylindrical cloak at an oblique angle. The transformation media that comprises the cloak lies in an annular region between the cylinders from [10].

One, hopefully, can see the nightmare that such a cloak would take to build, based on the anisotropic properties needed for the design. The equations seem simple. However, there are six parameters required to be tailored, which are all functions of the radius. Nonetheless, for a cloaking metamaterial solution, these are the properties necessary to yield an applicable solution to our problem in high-energy electromagnetic defense.

The next step is to simulate the model using the parameters identified in this section using the COMSOL multi-physics simulation program and analyze the results. Setting up the material properties of the cylindrical shell using the radius-dependent, anisotropic relative permittivity and permeability in COMSOL is not too

difficult, but it does require a coordinate transformation. In the previous section, we defined the material properties in cylindrical coordinates. However, the COMSOL solver requires Cartesian coordinates. We need to apply the standard coordinate transformations, for which the  $z$  components do not change:

$$\varepsilon_{xx} = \varepsilon_r \cos^2 \phi + \varepsilon_\phi \sin^2 \phi \quad (5.15)$$

$$\varepsilon_{xy} = \varepsilon_{yx} = (\varepsilon_r - \varepsilon_\phi) \sin \phi \cos \phi \quad (5.16)$$

$$\varepsilon_{yy} = \varepsilon_r \sin^2 \phi + \varepsilon_\phi \cos^2 \phi \quad (5.17)$$

with  $\overline{\overline{\mu}} = \overline{\overline{\varepsilon}}$  completes the tensor description. Applying these transformations to the material property cloak yields the following tensors to be used in defining the needed cloaking material parameters in the COMSOL interface:

$$\overline{\overline{\mu}} = \overline{\overline{\varepsilon}} = \begin{pmatrix} \left( \frac{r-a}{r} \right) \cos^2 \phi + \left( \frac{r}{r-a} \right) \sin^2 \phi & \left( \frac{r-a}{r} - \frac{r}{r-a} \right) \sin \phi \cos \phi & 0 \\ \left( \frac{r-a}{r} - \frac{r}{r-a} \right) \sin \phi \cos \phi & \left( \frac{r-a}{r} \right) \sin^2 \phi + \left( \frac{r}{r-a} \right) \cos^2 \phi & 0 \\ 0 & 0 & \left( \frac{b}{b-a} \right)^2 \frac{r-a}{r} \end{pmatrix} \quad (5.18)$$

with  $r = \sqrt{x^2 + y^2}$  and  $\phi = \arctan\left(\frac{y}{x}\right)$ .

## B. COMSOL SIMULATIONS

The following simulations show an incident Gaussian laser beam and a 2D cylindrical shell. The parameters for both have been described in earlier chapters. For the entirety of the simulations, the shown plane is the x-y plane with the z-component being outward normal to the plots. The electric field used in all simulations will be of the form,

$$\vec{E}(y, x) = E_0 \frac{w_0}{w(x)} \exp\left[-\frac{y^2}{w^2(x)}\right] \exp\left[-ikx + i \tan^{-1}\left(\frac{x}{x_R}\right) - \frac{iky^2}{2R(x)}\right] \hat{z} \quad (5.19)$$

where the wave is traveling in the positive x-direction, the amplitude falls off as a Gaussian in the y-direction, and the polarization is in the z-direction.

Figure 15 shows the background electric field that will be used incident upon the 2D cylindrical shell for the cloaking material solution.

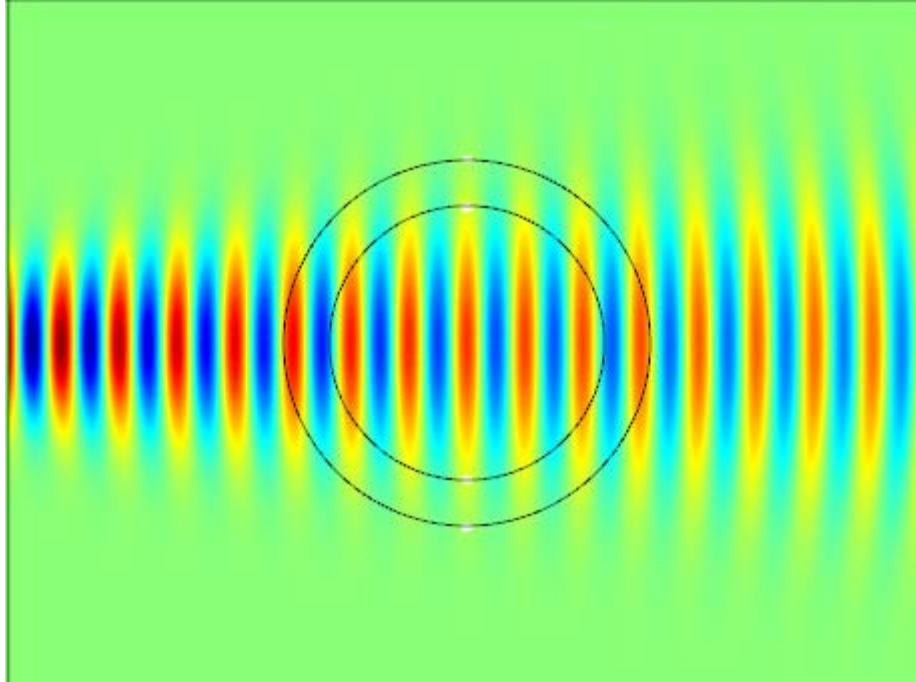


Figure 15. Shows the incident electric Gaussian beam which is used in the simulations.

Now that the field is set up, we need to apply the cloaking parameters to the shell, and test the theoretical material solution viability of our designed shell. After applying the properties to the shell and simulating the results, the following figures display the results.

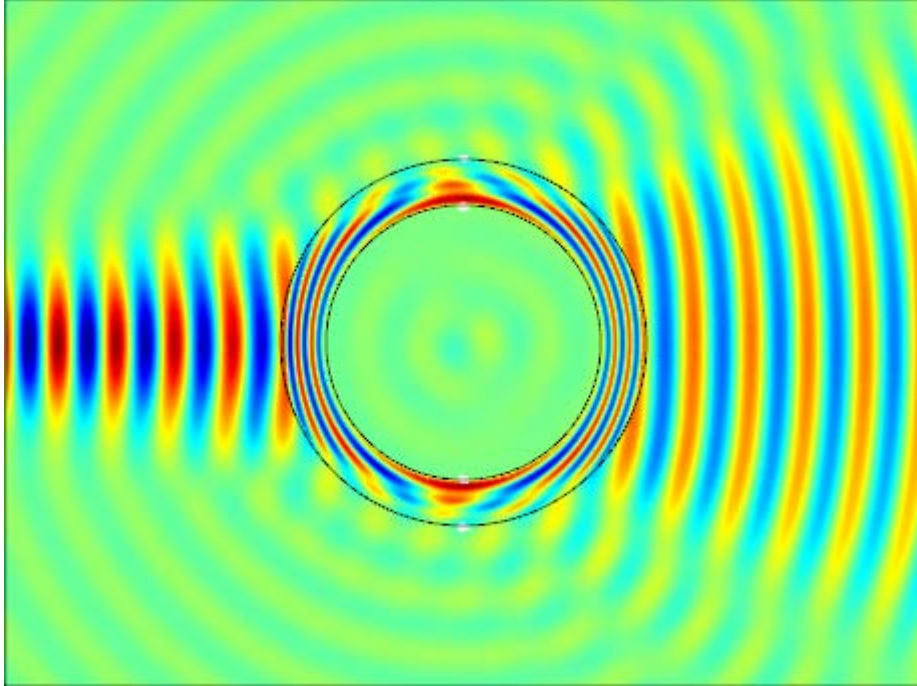


Figure 16. Z-component of the resulting electric field for the 2D cloaked cylindrical shell.

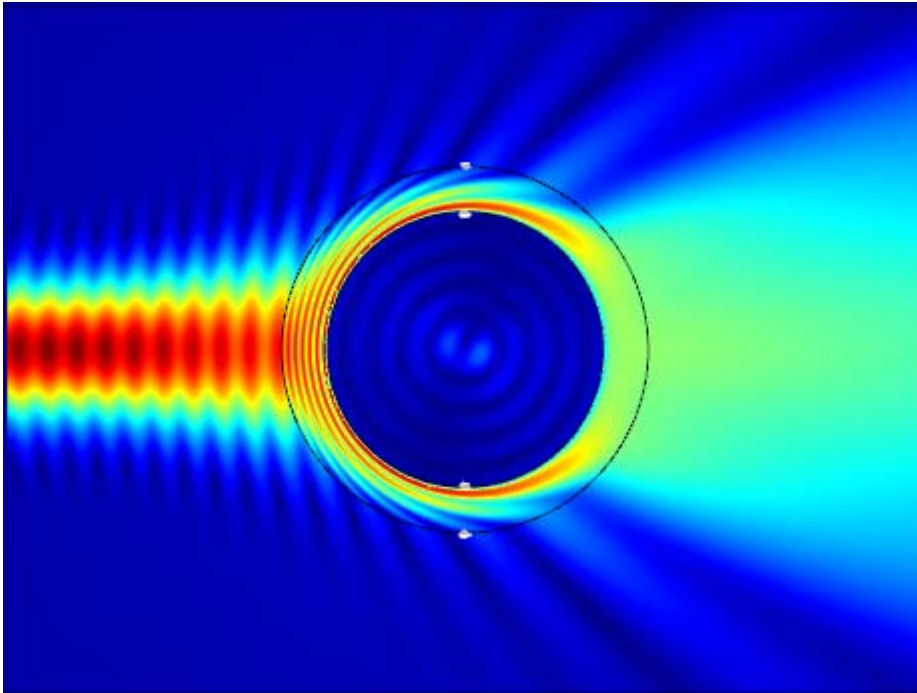


Figure 17. Electric field magnitude for the 2D cloaked cylindrical shell.

The simulation reveals that the incident wave is not fully cloaked. The reasoning for this is not an error within the formulation of the applied cylindrical cloak, but in using the approximated 2D Gaussian laser beam in the model. The issue was briefly described in Chapter IV while formulating a suitable electric field as an input laser beam. The result is that the COMSOL RF solver has to most effectively solve for Maxwell's equations given an input wave that does not satisfy them. As a result, the cylindrical layer does not fully cloak, which is noticeably seen in the simulation by the electric field changing due to the interaction within the layer. However, this is not an entirely significant issue based on the nature of the thesis topic. As already stated, perfect invisibility is not a required constraint, and not something that needs to be shown. What has been illustrated by the above simulation is that applying a cylindrical cloaking layer does theoretically redirect the incident approximated electric field around the core as desired. A plane wave simulation that depicts a cloaking solution is illustrated in the Appendix.

Next, to have a more complete understanding of our proposed cloaking material solution, the Gaussian beam will be shifted to explore the resulting electric field from different geometries of incidence.



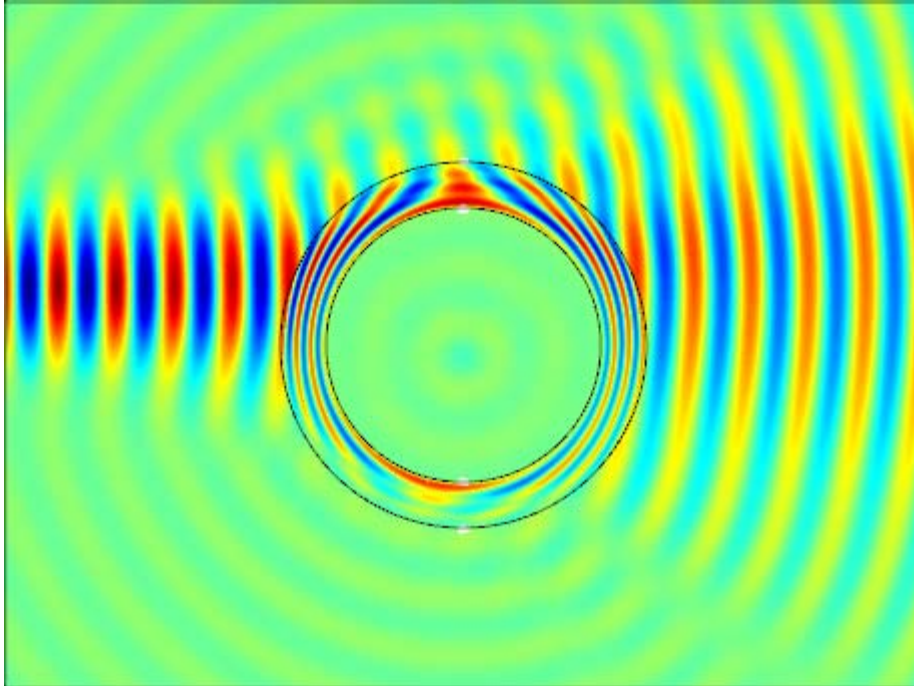


Figure 18. Shifted 0.05 cm. Z-component of the electric field for the 2D cloaked cylindrical shell.

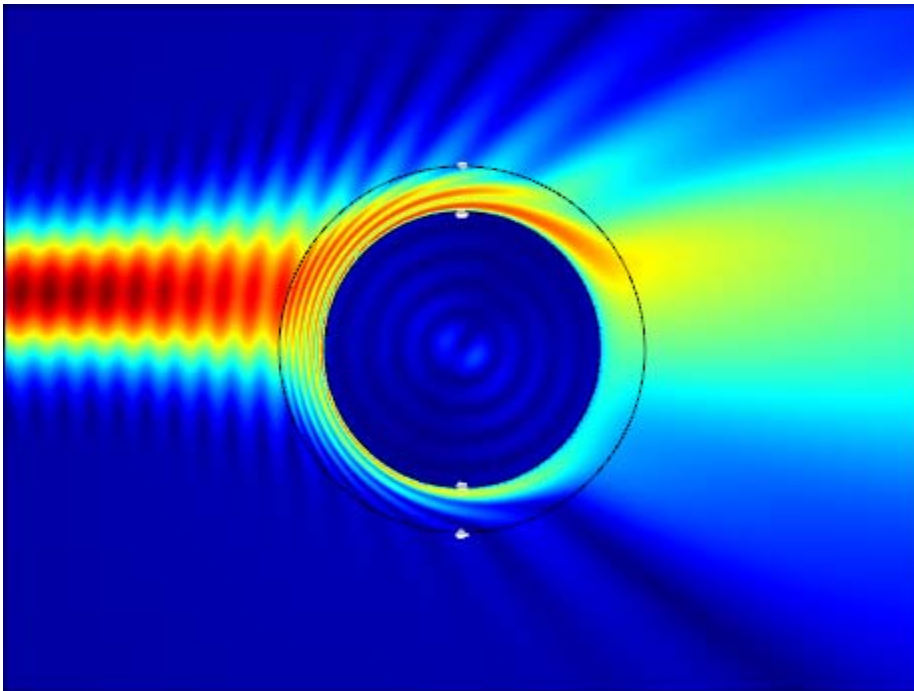


Figure 19. Shifted 0.05 cm. Electric field magnitude for the 2D cloaked cylindrical shell.

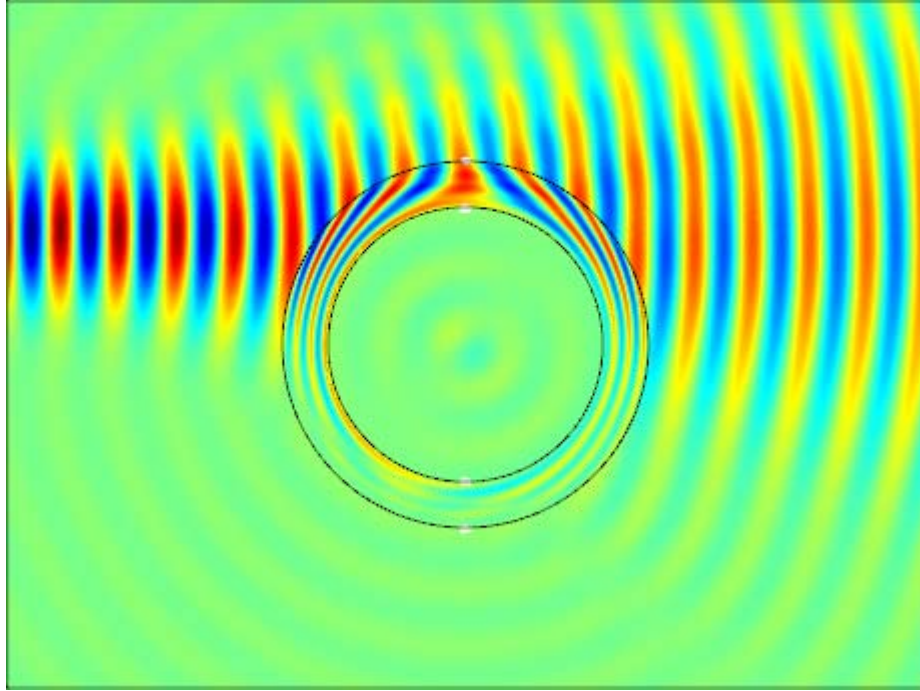


Figure 20. Shifted 0.1 cm. Z-component of the electric field for the 2D cloaked cylindrical shell.

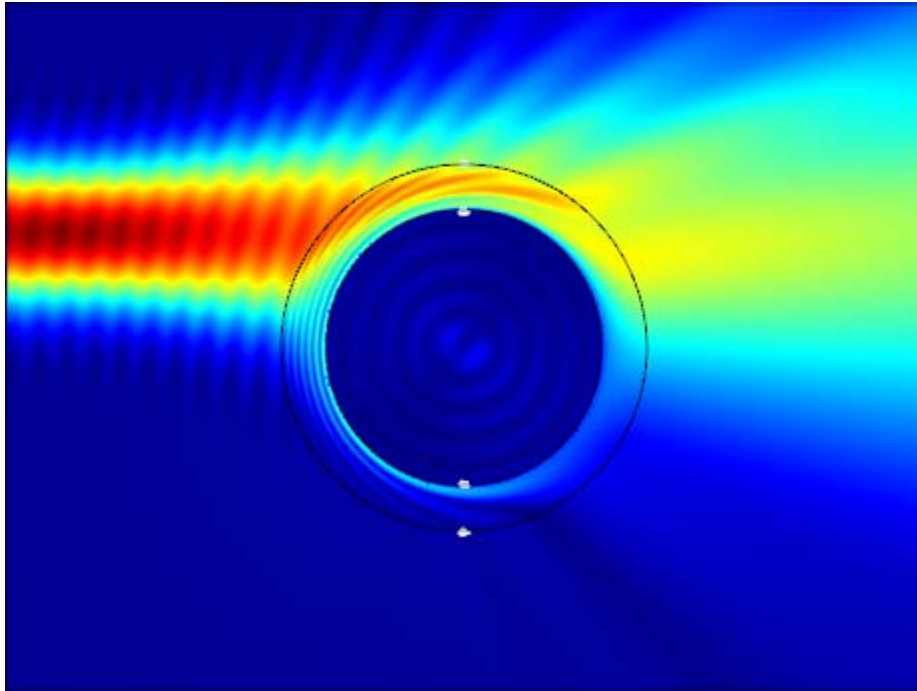


Figure 21. Shifted 0.1 cm. Electric field magnitude for the 2D cloaked cylindrical shell.

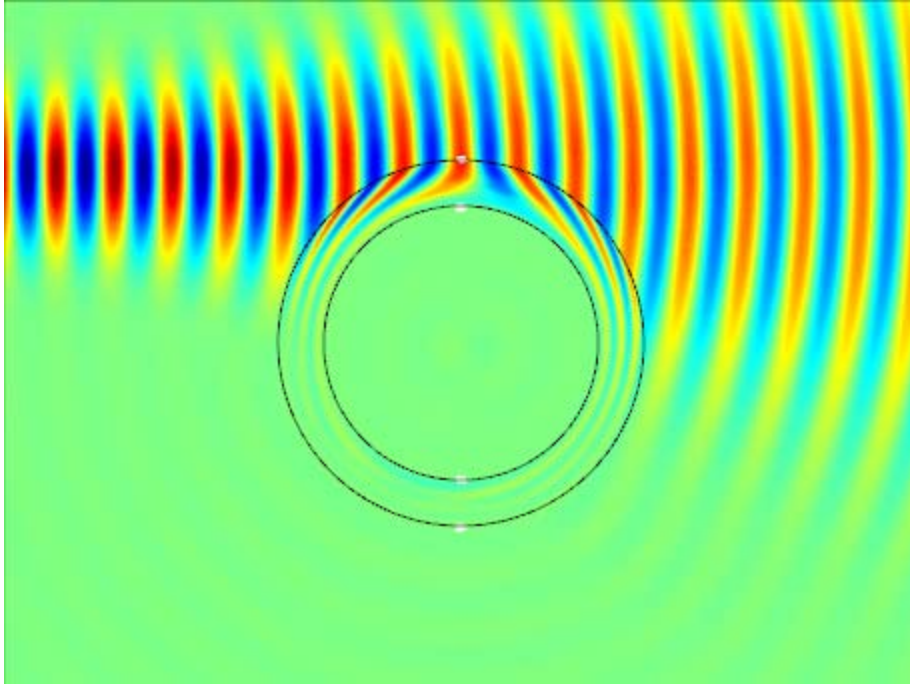


Figure 22. Shifted 0.15 cm. Z-component of the electric field for the 2D cloaked cylindrical shell.

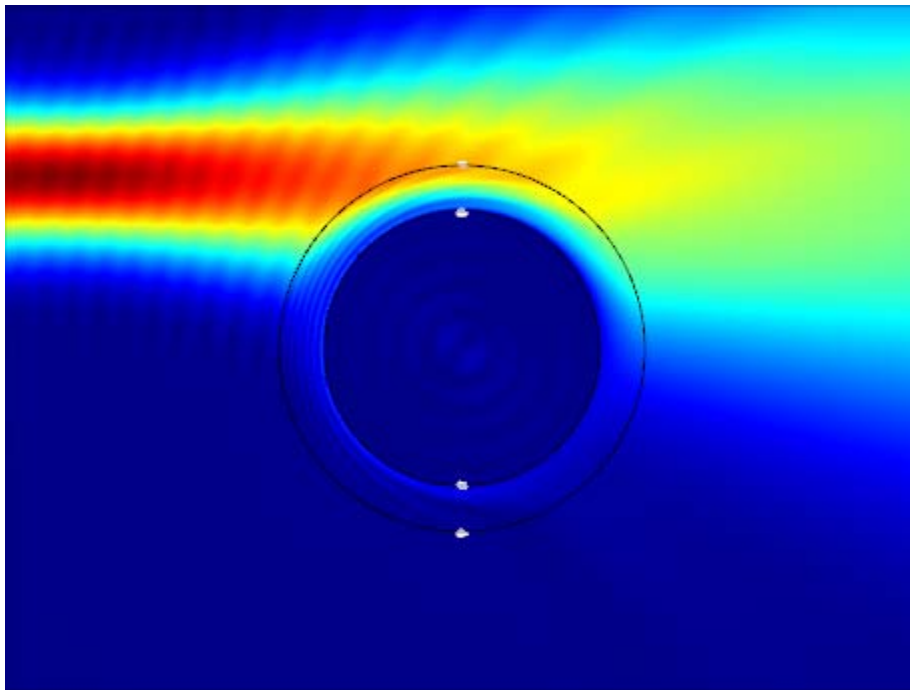


Figure 23. Shifted 0.15 cm. Electric field magnitude for the 2D cloaked cylindrical shell.

The above figures illustrate that the proposed cloaking material solution theoretically protects the core from the modeled laser beam regardless of the offset from normal incidence.

## **VI. CYLINDRICAL DEFLECTION MATERIAL SOLUTION**

### **A. SOLUTION SETUP**

The proposed material solution for a simple deflection layer around the missile is the exact same model setup as the cloaking problem formulation, with the exception that we will be defining the material layer solution to have material properties that are isotropic within the layer. The COMSOL environment allows us to make these changes to our existing models that were used in the previous chapter.

To get the best-proposed solution, we first use a plane wave incident on the cylindrical shell to test the material solution for various material properties, to ascertain which values yield better deflection results for a proposed C-DEW material solution. After selecting the best-proposed solution parameters, we display the simulations using the modeled laser at various beam incidences.

### **B. COMSOL SIMULATIONS**

The following simulations show an incident plane wave and a 2D cylindrical shell. Parameters are the same as in previous chapters. With a plane wave, one can see the total resultant field more clearly than when a Gaussian beam is employed. Once optimal material properties are found, we will return to using an incident Gaussian laser beam. Trial and error is used to hone in on a preferred material solution.

For the entirety of the simulations, propagation is in the x-y plane, with the z-component being outward normal to the plots. The electric field used in all plane wave simulations is of the form

$$\vec{E}(y, x) = E_0 \exp[-ikx] \hat{z} \quad (6.1)$$

where the plane wave is traveling in the positive x-direction and the polarization is in the z-direction. The incident plane wave is shown below.

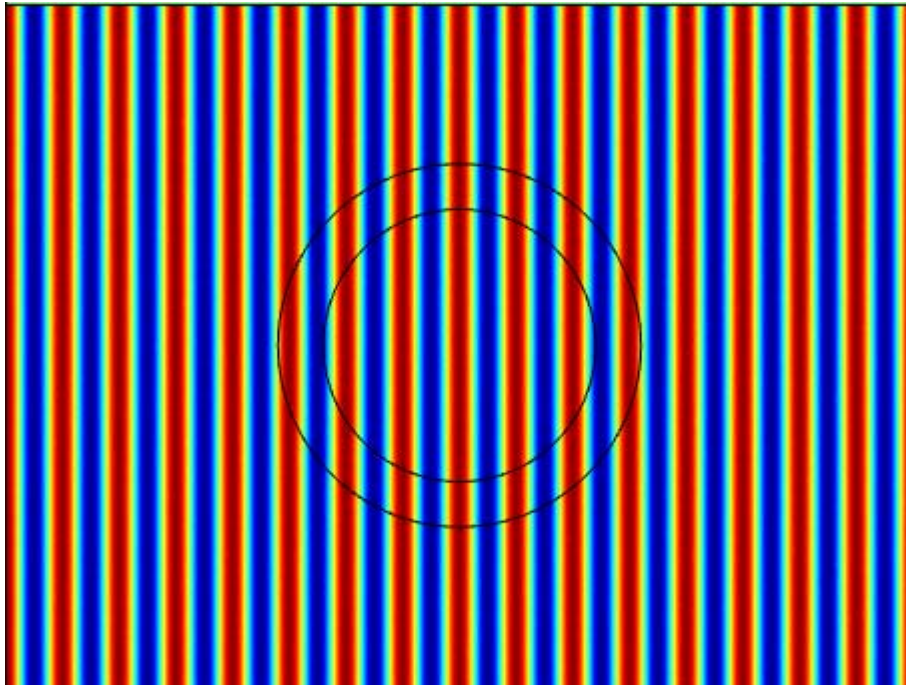


Figure 24. Shows the incident electric plane wave that is used in the simulations.

To test for the best possible solution, the permeability ( $\mu$ ) and permittivity ( $\epsilon$ ) are varied. To limit the parameter space we keep both parameters isotropic and equal throughout the cylindrical layer. The goal is to analyze the resulting fields for different values of these



parameters, and to determine which values would, in theory, yield a better C-DEW material solution. Results are shown for various parameters for the cylindrical shell. The z-component of the resulting electric field is shown as a result of various proposed 2D deflection cylindrical shell material solutions.

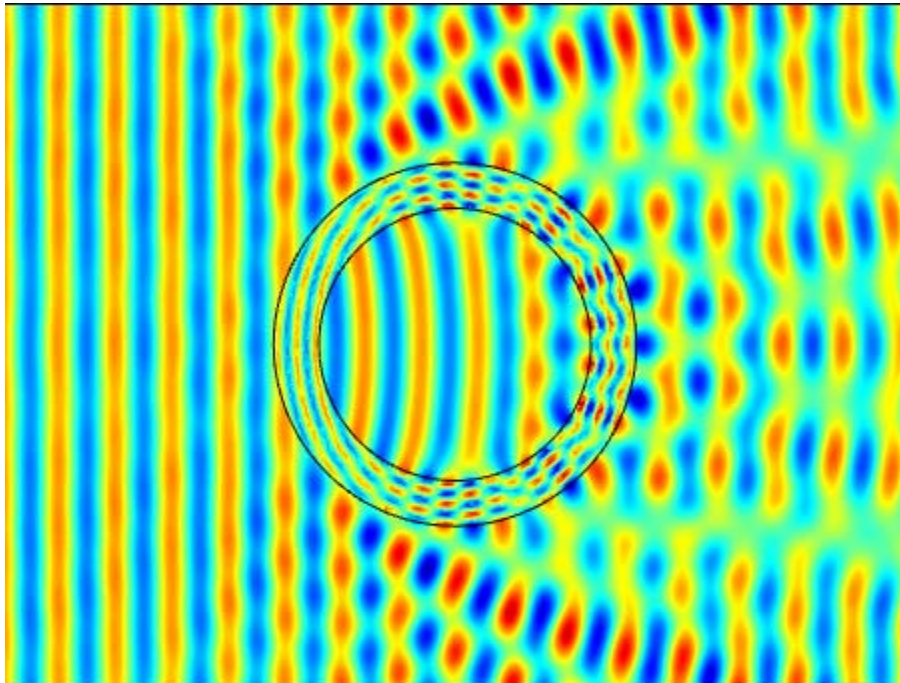


Figure 25.  $\epsilon = \mu = 3$ . Z-component of the resulting electric field for the 2D cylindrical shell.

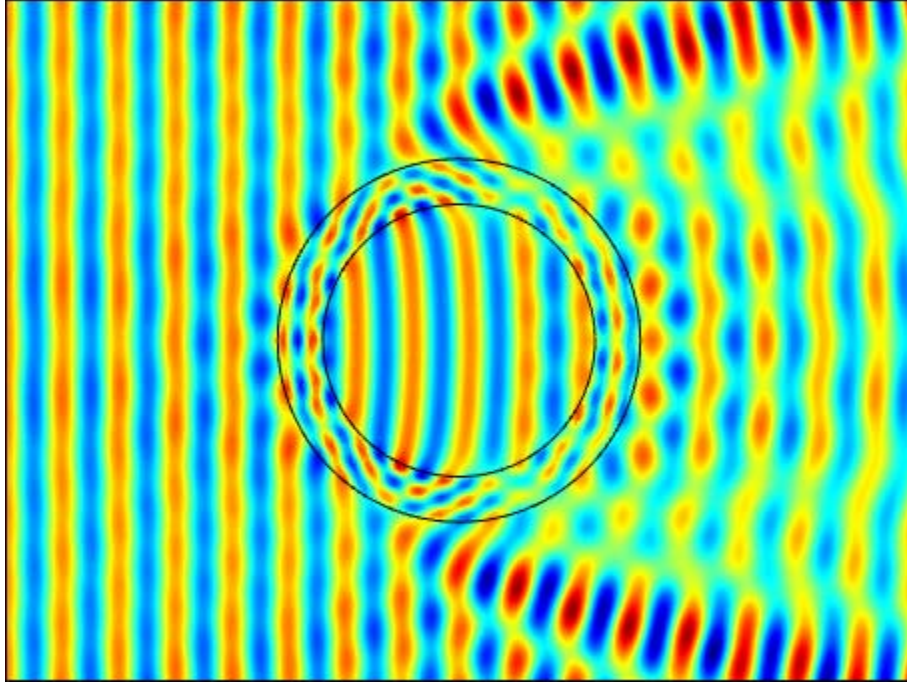


Figure 26.  $\varepsilon=\mu=2$ . Z-component of the resulting electric field for the 2D cylindrical shell.

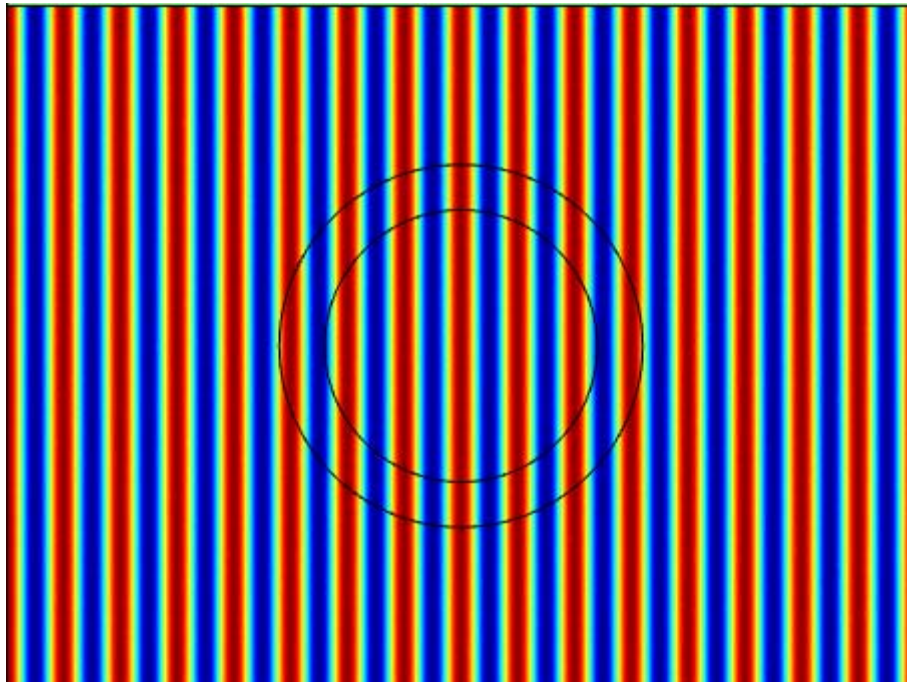


Figure 27.  $\varepsilon=\mu=1$ . Z-component of the resulting electric field for the 2D cylindrical shell.



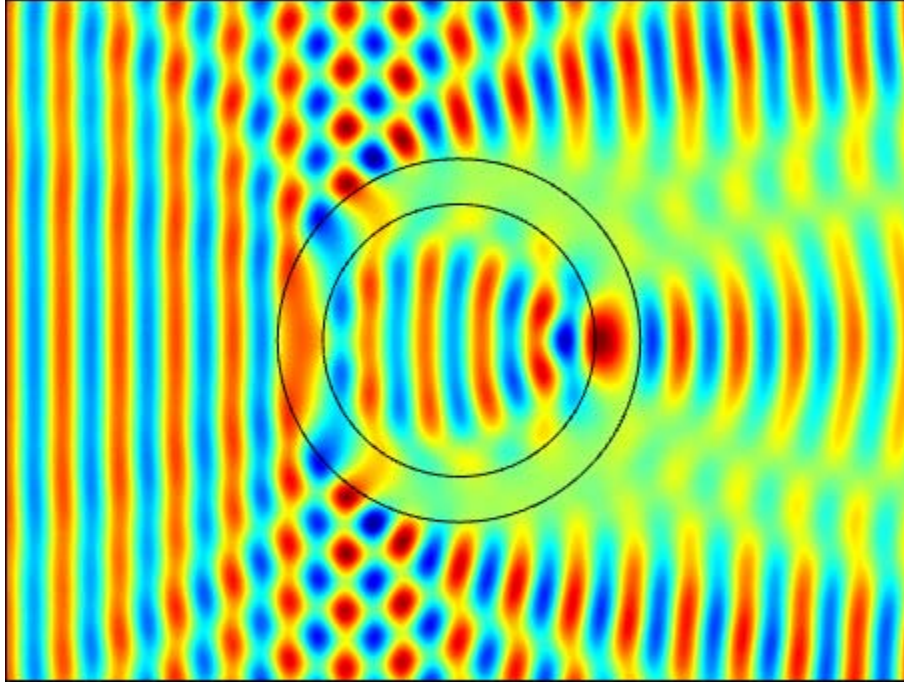


Figure 28.  $\epsilon = \mu = 0.5$ . Z-component of the resulting electric field for the 2D cylindrical shell.

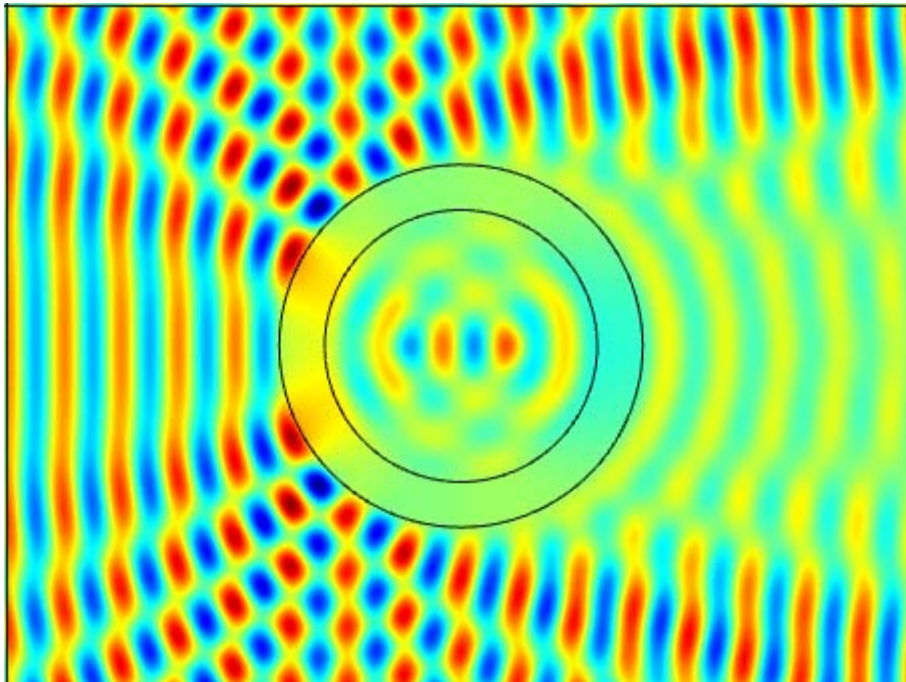


Figure 29.  $\epsilon = \mu = 0.1$ . Z-component of the resulting electric field for the 2D cylindrical shell.

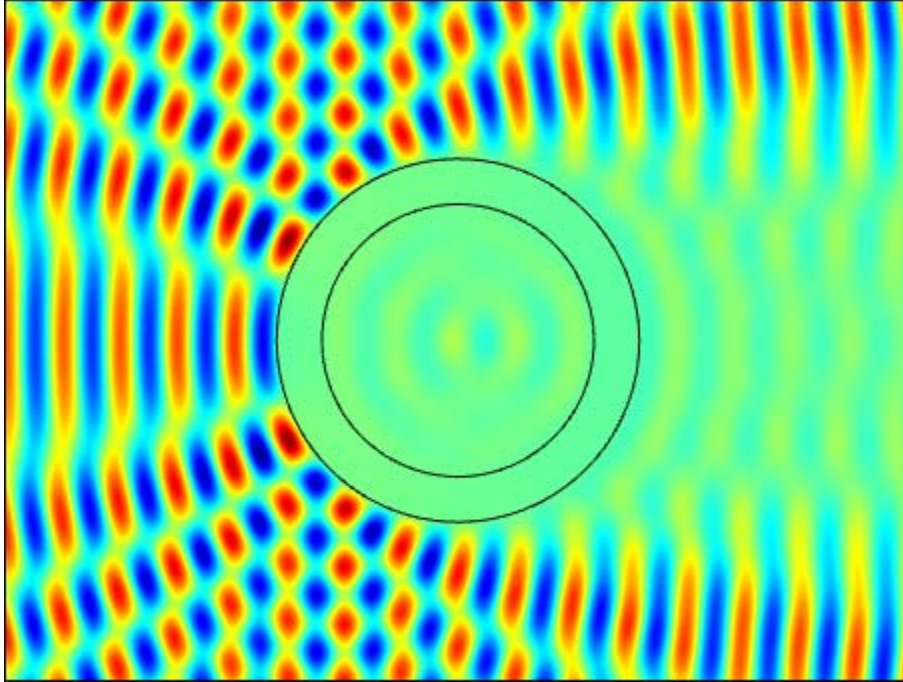


Figure 30.  $\epsilon = \mu = 0.01$ . Z-component of the resulting electric field for the 2D cylindrical shell.

We can see that the best proposal for a deflective material solution is one in which the permeability ( $\mu$ ) and permittivity ( $\epsilon$ ) have values less than one and limiting towards zero. The remainder of the simulations use the modeled Gaussian laser beam, with  $\epsilon = \mu = 0.01$ , to explore the fields resulting from the cylindrical shell at various incidences.

The following simulations show an incident Gaussian laser beam and a 2D cylindrical shell. The parameters for both have been described in earlier chapters. For the entirety of the simulations, the shown plane is the x-y plane, with the z-component being outward normal to the plots. The electric field used in all simulations will be of the form,

$$\bar{E}(y, x) = E_0 \frac{w_0}{w(x)} \exp\left[-\frac{y^2}{w^2(x)}\right] \exp\left[-ikx + i \tan^{-1}\left(\frac{x}{x_R}\right) - \frac{iky^2}{2R(x)}\right] \hat{z} \quad (6.2)$$

where the wave is traveling in the positive x-direction, the amplitude falls off as a Gaussian in the y-direction, and is polarized in the z-direction.

The following figure shows the background electric field, which will be used incident upon the 2D cylindrical shell for the deflection material solution.

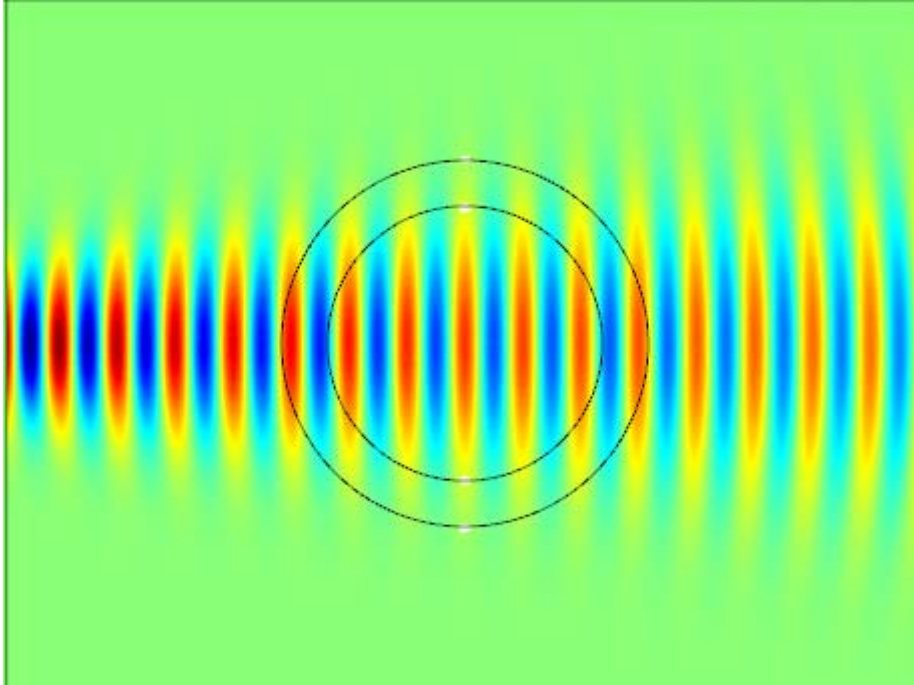


Figure 31. Shows the incident Gaussian beam that is used in the deflection material solution simulations.

Next, the following figure shows the results of the simulation for the incident Gaussian laser beam incident upon the cylindrical shell material solution for the values of  $\varepsilon = \mu = 0.01$ .

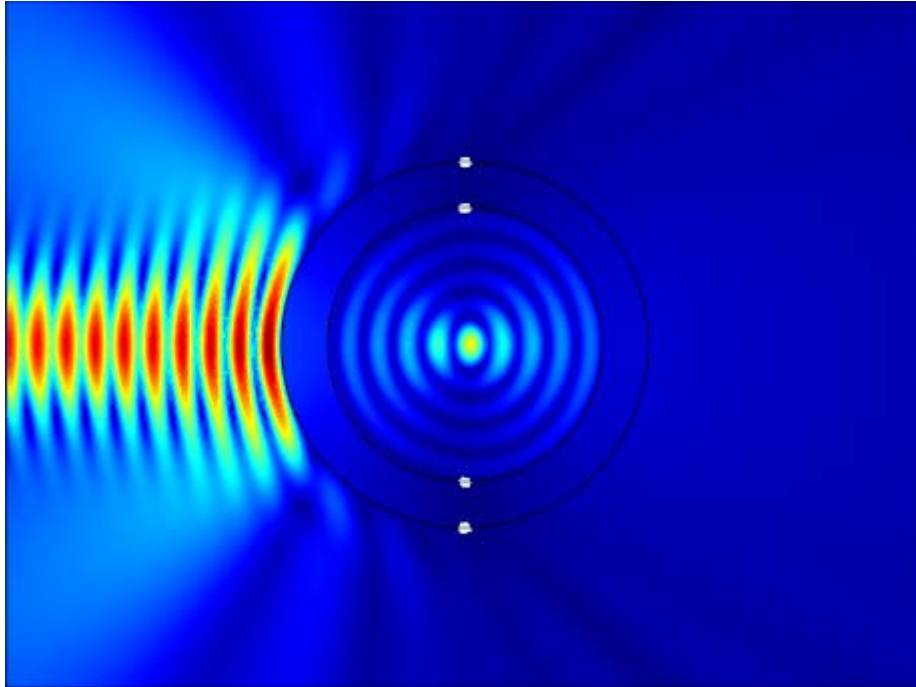


Figure 32.  $\varepsilon = \mu = 0.01$ . Resulting electric field magnitude for the 2D cylindrical shell.

As expected from the above plane wave simulations, the deflection material solution is able to mostly protect the inner core from the incident electric field radiation under normal incidence.

Next, to have a more complete understanding of our proposed deflection material solution, the Gaussian beam will be shifted so that we can explore the resulting fields from different geometries of incidence.

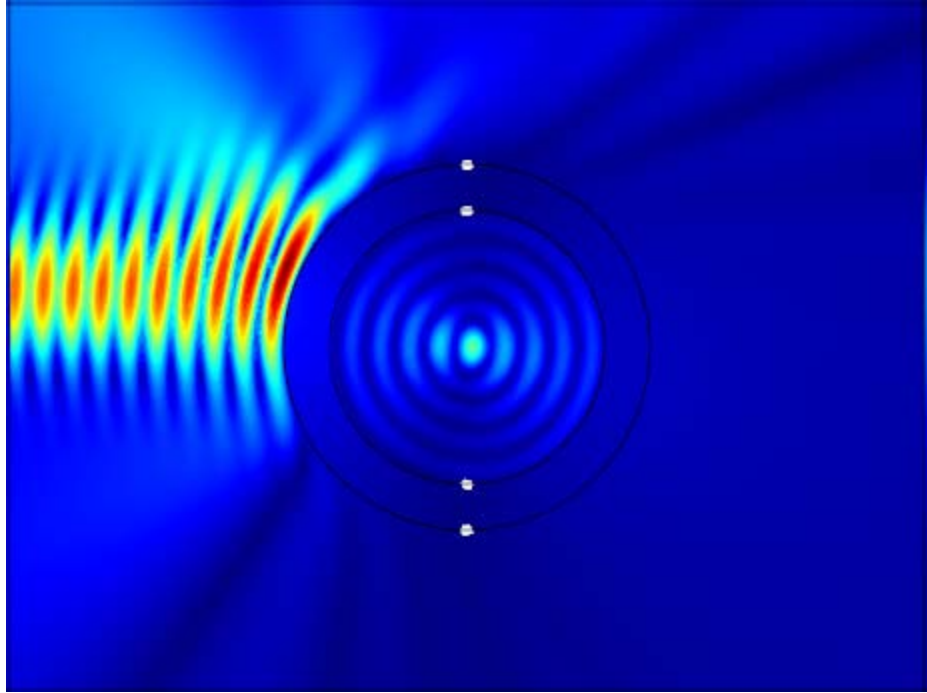


Figure 33.  $\varepsilon = \mu = 0.01$ . Shifted 0.05 cm. Resulting electric field magnitude for the 2D cylindrical shell.

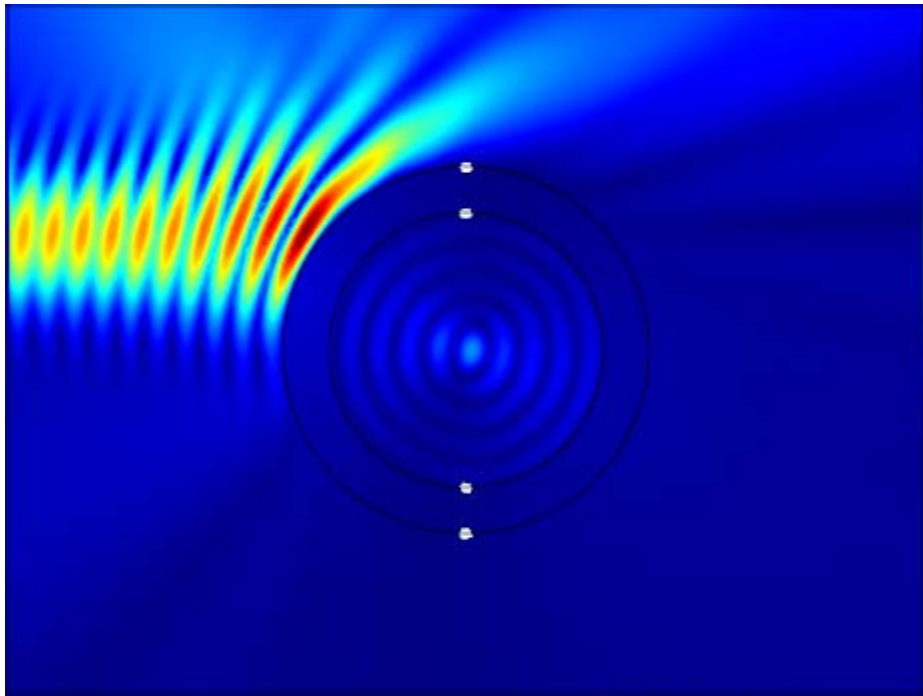


Figure 34.  $\varepsilon = \mu = 0.01$ . Shifted 0.1 cm. Resulting electric field magnitude for the 2D cylindrical shell.



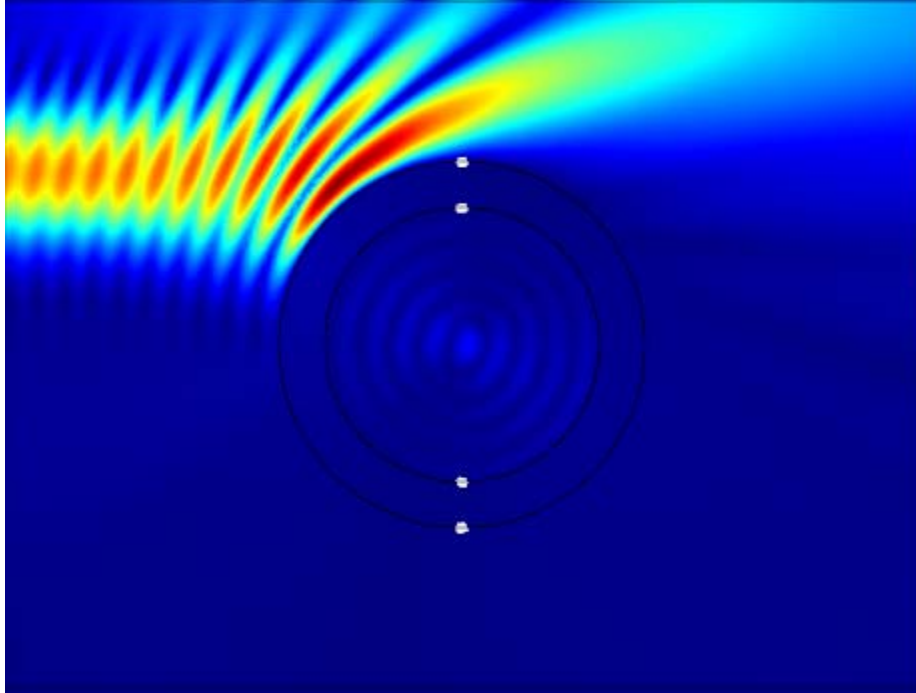


Figure 35.  $\epsilon = \mu = 0.01$ . Shifted 0.15 cm. Resulting electric field magnitude for the 2D cylindrical shell.

The above figures illustrate that the proposed deflection material solution theoretically gets better at protecting the core as the offset from normal incidence increases.

## VII. CONCLUSIONS

### A. FINDINGS

The COMSOL Multiphysics package proved to be an invaluable tool for simulating the theoretical idea of using metamaterials as a proposed material solution to the problem of C-DEW defense in the specific case of a high-energy electromagnetic weapon. The purpose of this thesis was to set up the entire problem from start to finish, and then model it using the COMSOL environment. That goal was most certainly met, and I believe, through the simulation findings, there has been a definite case made for further research in the area.

The simulations for the proposed cloaking material solution did not illustrate a perfect cloak by the layer as a result of the approximated electric field used as an input. However, due to the nature of the problem and the results desired, this was not necessary to show. The difference between the simulations in this thesis and what is prevalent in current research on cloaking, is the application for which the cloak would be used. Near perfect invisibility is not necessary for the present application. In C-DEW defense, the main goal is to build a material solution that would protect an asset from a DEW threat. Analyzing the simulation plots shows that for the proposed cloaking material solution, the cloaking layer was able to redirect electromagnetic radiation incident upon the cylinder through the cloaking layer, and away from the core

at various incidences. The simulation plots provide a great pictorial view of the resulting theoretical effectiveness of such a material solution.

As for the proposed deflection material solution, one can also see from the simulations that by tuning the permeability ( $\mu$ ) and permittivity ( $\epsilon$ ) towards unnaturally occurring small values, one arrives at a solution in which a material could be manufactured as a skin layer capable of deflecting the radiation away from the core, and more importantly, the entire missile. The advantage of such a material solution, when compared to a cloaking layer, is that there is less radiation penetration into the missile. Radiation penetration within the defensive material layer needs to be minimized in order to reduce energy conversion to heat.

From a completely theoretical sense, both material solutions seem to have promise. Both material solutions have been shown in the simulations to redirect electromagnetic radiation away from sensitive components in a cylindrical geometry. However, in protecting from an actual C-DEW threat, future realistic feasibility studies relating to the construction and viability under intense radiation of such metamaterials will need to be discussed further.

## **B. MATERIAL SOLUTIONS LIMITATIONS**

Both material solutions have their limits. This thesis is grounded upon a very basic research emphasis towards an interest of the ONR. While hypothetical, the problem is likely to develop and will require further research in various fields of physics, engineering, and material



science. Constraints, have been glossed over, in defining our models, and some have yet to be discussed, but must be addressed. While the theoretical solutions presented look highly interesting, there are realistic limitations. Addressing some of these concerns is a good next step. Knowledge of these challenges and the viability of the material solutions presented must be based on actual real world constraints.

The challenges of finding usable solutions to the material solutions are considerable. A proposed FEL weapon would project energy on the order of a megawatt. Currently, metamaterials are very "lossy." It means that a lot of the energy travelling through the layer will be absorbed as heat. A cloaking material solution would be affected by this considerably. Further research will need to be done in engineering highly efficient metamaterials that are capable of withstanding significant amounts of heat energy before one could ever imagine a cloaking metamaterial layer that could redirect a high-energy laser beam such as a FEL. Further problems arise in the complexity of metamaterial construction given that with a cloaking layer six parameters must be tailor-fit, and are continuously changing throughout the layer. A third limitation of the cloaking solution for C-DEW defense is that the entire cloak is typically designed for a very specific wavelength of incident radiation. One of the design features of a FEL, as was previously stated, is its tuning ability. Changing the incident frequency could therefore render a non-variable cloaking layer ineffective to all but a very narrow band of frequencies. Cloaking is a very interesting and exciting topic, but, in C-DEW defense, due to the material anisotropic constraints, current

metamaterial inefficiencies, and the narrow band gap of effectiveness, I do not think it is a technique worthy of further research.

As for a deflection material solution, there are limits as well. Again, manufacturing of complex material structures is difficult, and that is why, for simplicity the proposed material solution parameters were kept isotropic and equal throughout. The advantage of a deflective medium solution is that radiation energy passing through any part of the cylinder would be minimized. Keeping high-energy radiation out of the cylinder, is, by far, the more logical step towards envisioning a possible C-DEW material solution. Again, with such a metamaterial solution, one concludes that metamaterials are designed for a narrow band of frequencies. With the solution presented, however, one could imagine a material solution layer being composed of cylindrical shells of various metamaterial configurations, to better defend against a wider band of frequencies.




In the end, both metamaterial solutions have theoretical viability, which has been demonstrated by the COMSOL simulations presented in this thesis. However, at present time metamaterial efficiency, manufacturing techniques, and most importantly, narrow band effectiveness limits their potential for use towards the problem of C-DEW defense. However, I do think that further research into an isotropic shell composed of various metamaterial configurations is worth researching and eventually testing using a high-energy laser. Research into the actual

empirical bandwidth size for certain types of metamaterial configurations would give a conclusive determination of viability.

THIS PAGE INTENTIONALLY LEFT BLANK

## APPENDIX. MODELING AND SIMULATION TUTORIAL FOR COMSOL 4.0

### MODEL WIZARD

1. Start COMSOL by double-clicking its icon on the desktop.
2. When the **Model Wizard** opens, select the **2D** space dimension. Click the **Next** button  to continue to the Physics page.
3. In the **Add Physics** step, click the **Radio Frequency** folder, right-click **Electromagnetic Waves (emw)** and **Add Selected**. Click the **Next** button .
4. The last **Model Wizard** step is to select **Study Type**. Select the **Boundary Mode Analysis** study type and click the **Finish** button .

### GLOBAL DEFINITIONS

5. Right-click **Global Definitions** and select **Parameters** to create a list of parameters. In the **Parameters** field enter the following:

<u>Name</u>	<u>Expression</u>	<u>Description</u>
lam	0.05[m]	Wavelength
freq	c_const/lam	Frequency
per_R	0.25	Material Sol. Thickness Coefficient
R2	0.16[m]	Outer Cylinder Radius
R1	R2*(1-per_R)	Inner Cylinder Radius

### VARIABLES

6. Under the **Model 1 (mod1)** tree, Right-click **Definitions** and select **Variables** to create a list of variables to be used for both the cloak and isotropic material solutions. Enter the list below in the appropriate fields.

<u>Name</u>	<u>Expression</u>
r	$\sqrt{x^2+y^2}$
phi	$\text{atan}(y/x)$
e_r	$(r-R1)/r$

```


e_phi      r/(r-R1)
e_xx      e_r*cos(phi)^2+e_phi*sin(phi)^2
e_xy      (e_r-e_phi)*sin(phi)*cos(phi)
e_yy      e_r*sin(phi)^2+e_phi*cos(phi)^2
e_zz      ((R2/(R2-R1))^2)*((r-R1)/r)
e_ind      .01
u_ind      e_ind

```

## BUILD GEOMETRY

7. Under the **Model 1 (mod1)** tree, Right-click **Geometry 1** and select **Circle** or **Rectangle** and create the list of objects defined below using the following specifications:


- Circle, Radius: R1, Base: Center, x: 0, y: 0
- Circle, Radius: R2, Base: Center, x: 0, y: 0
- Rectangle, Width: 0.8, Height 0.6, Base: Center, x: 0, y: 0
- Rectangle, Width: 1, Height 0.1, Base: Corner, x: -0.5, y: 0.3
- Rectangle, Width: 1, Height 0.1, Base: Corner, x: -0.5, y: -0.4
- Rectangle, Width: .1, Height .8, Base: Corner, x: -0.5, y: -0.4
- Rectangle, Width: .1, Height .8, Base: Corner, x: 0.4, y: -0.4

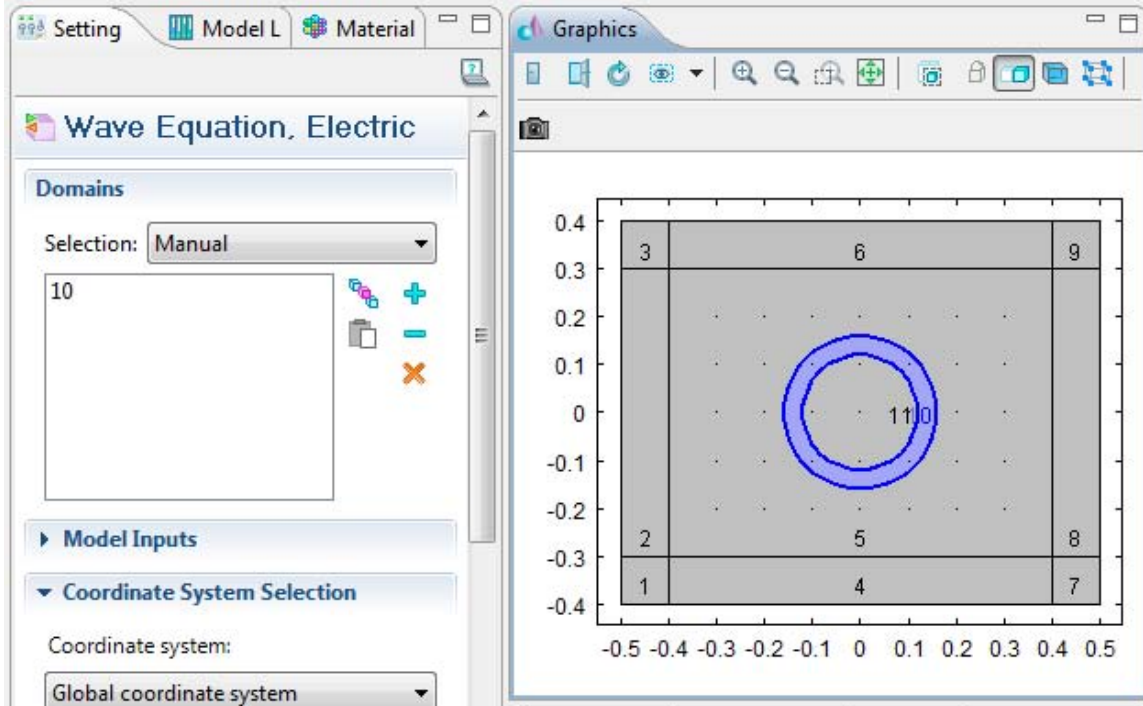
Click the **Build All** button  when complete.

## ADD PHYSICS

7. Under the **Model 1 (mod1)** tree, select **Electromagnetic Waves (emw)**. In the fields select the following:

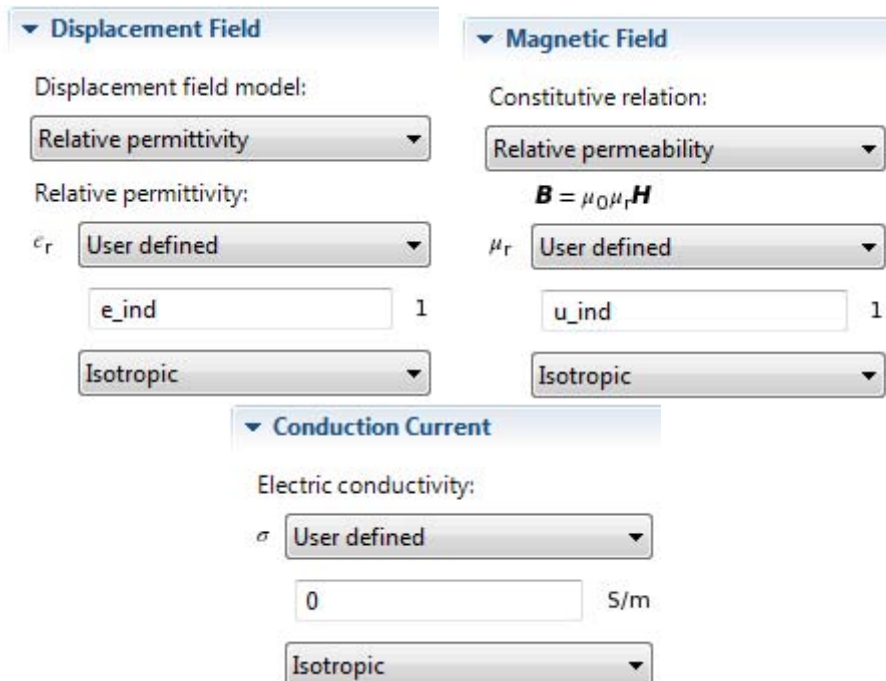
Electric field components solved for: Three-component vector  
 Solve for: Scattered field  
 Background electric field:  $E_x=0, E_y=0, E_z=\exp(-j*emw*k_0*x)$

8. Right-click **Electromagnetic Waves (emw)** and select **Wave Equation, Electric**. Under the **Electromagnetic Waves (emw)** tree select the newly created **Wave Equation, Electric 2**. On your model left click on the region between the two circles and click the plus  button.



9. Now for this layer we want to setup the material properties for either material solution (pick one or the other).

Deflecting Material Solution Specifications:



Cloaking Material Solution Specifications:

**Displacement Field**

Displacement field model:

Relative permittivity:  
 $\epsilon_r$

$\epsilon_{xx}$	$\epsilon_{xy}$	0
$\epsilon_{xy}$	$\epsilon_{yy}$	0
0	0	$\epsilon_{zz}$

1

**Magnetic Field**

Constitutive relation:

$\mathbf{B} = \mu_0 \mu_r \mathbf{H}$

$\mu_r$

$\mu_{xx}$	$\mu_{xy}$	0
$\mu_{xy}$	$\mu_{yy}$	0
0	0	$\mu_{zz}$

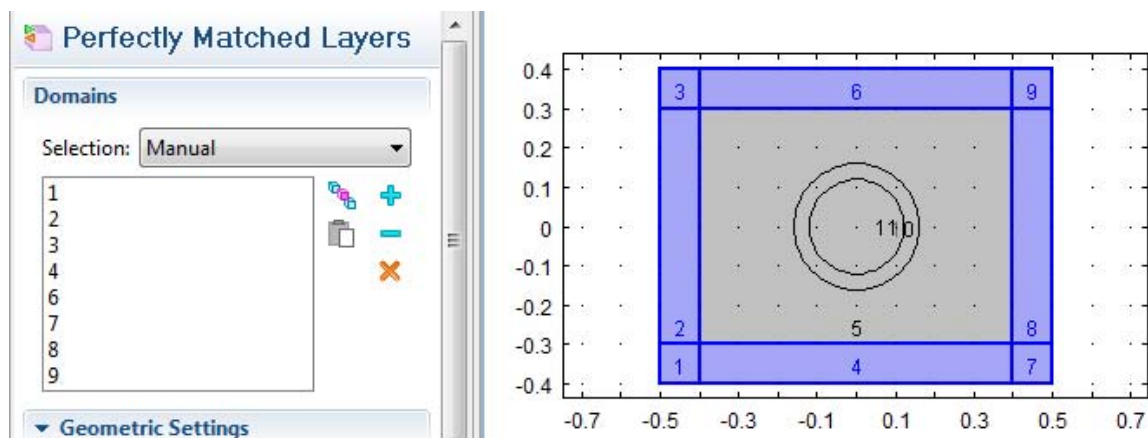
1

**Conduction Current**

Electric conductivity:  
 $\sigma$

S/m

10. Right-click **Electromagnetic Waves (emw)** and select **Perfectly Matched Layers**. Select all the outer boundary squares and rectangles in your model by shift clicking them. After selecting all of them click the plus **+** button in the **Domain** field.





11. Next, under the **Perfectly Matched Layers** tab, select **Wave Equation, Electric 1**. And set the following values for the layers.

The image shows three panels of settings for an electromagnetic simulation. The first panel, 'Displacement Field', has 'Displacement field model' set to 'Relative permittivity', 'Relative permittivity' set to 'User defined' with a value of 1, and 'Isotropic' selected. The second panel, 'Magnetic Field', has 'Constitutive relation' set to 'Relative permeability', the equation  $B = \mu_0 \mu_r H$  displayed, 'Relative permeability' set to 'User defined' with a value of 1, and 'Isotropic' selected. The third panel, 'Conduction Current', has 'Electric conductivity' set to 'User defined' with a value of 0 S/m, and 'Isotropic' selected.

As you should notice these values constitute the values that define a vacuum. We will use these same values again in the next step.

12. Under the **Electromagnetic Waves (emw)** tree select the **Wave Equation, Electric 1**. All that should be left selected is everything other than the material layer and the outer **Perfectly Matched Layers**. Set the same vacuum parameters from the previous step.

13. Right-click the **Electromagnetic Waves (emw)** and select **Scattering Boundary Condition**. Select all the very outer most line segments on the model and click the plus **+** button.

## MESHING

14. Under the **Mesh 1** tab select **Size**. Set the following:


Element Size: Custom  
 Maximum Element Size:  $\lambda_{\text{m}}/8$

We want our mesh to be much smaller than the wavelength of the incident electric field.

15. Right-click **Mesh 1**, and select **Free Triangular**. Repeat this step so that you have both a **Free Triangular 1** and a **Free Triangular 2** tab.

16. Click **Free Triangular 2** and in the **Geometry entity level** field select **Domain**. Select the material layer and click the plus **+** button. For both the **x-direction** and **y-direction scale** fields put **5** (ONLY set to 5 if you are doing the Cloaking Material Solution, if not, leave these values at 1). In the **Triangulation Method** field set it to **Delaunay**.

17. Click **Free Triangular 1** and in the **Geometry entity level** field select **Domain**. Select everything but the material layer and click the plus **+** button. For both the **x-direction** and **y-direction scale** fields put leave them at **1**. In the **Triangulation Method** field set it to **Delaunay**.

18. Click the Build All button  to mesh the model.

## STUDY

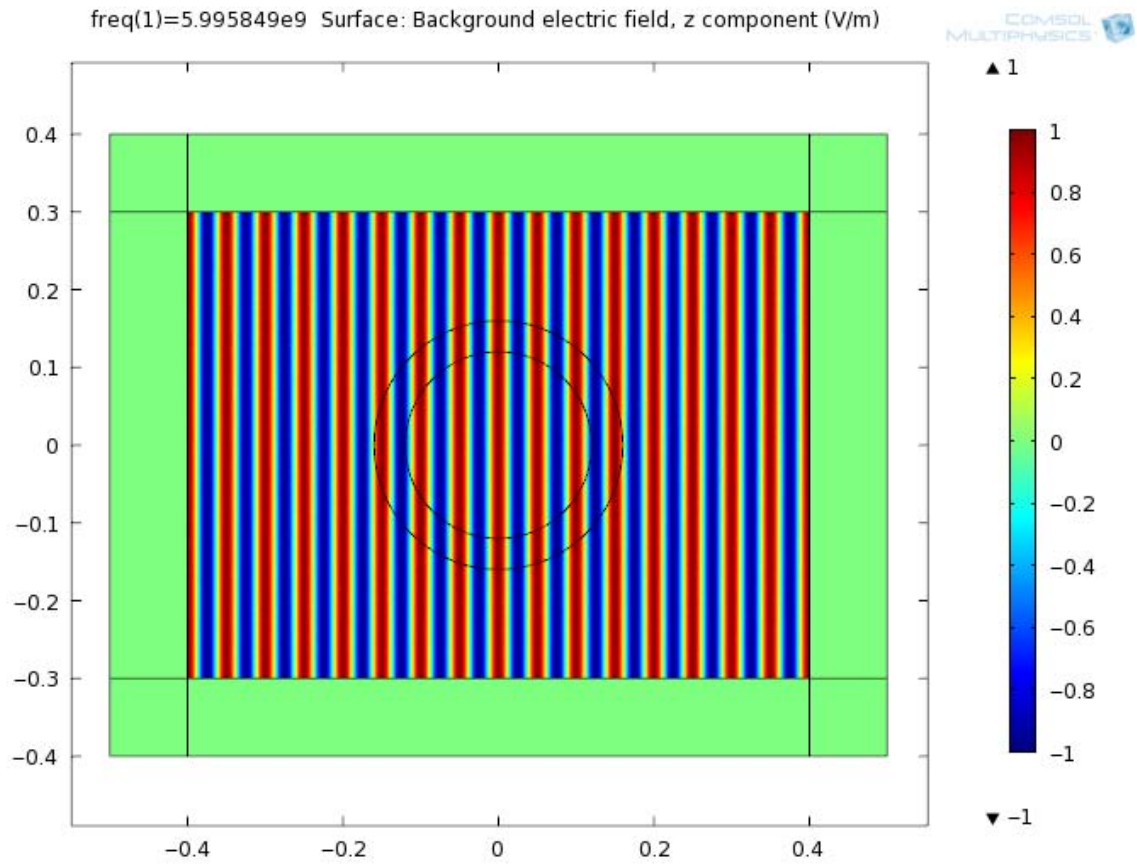
19. Click **Study 1**. Next we have to set frequency for the studies. Select **Step1: Boundary Mode Analysis** and set the **Mode analysis frequency** field to "freq". Next, select **Step1: Boundary Mode Analysis** and set the **Frequencies** field to "freq".

20. Right-click **Study 1** and select **Compute**.

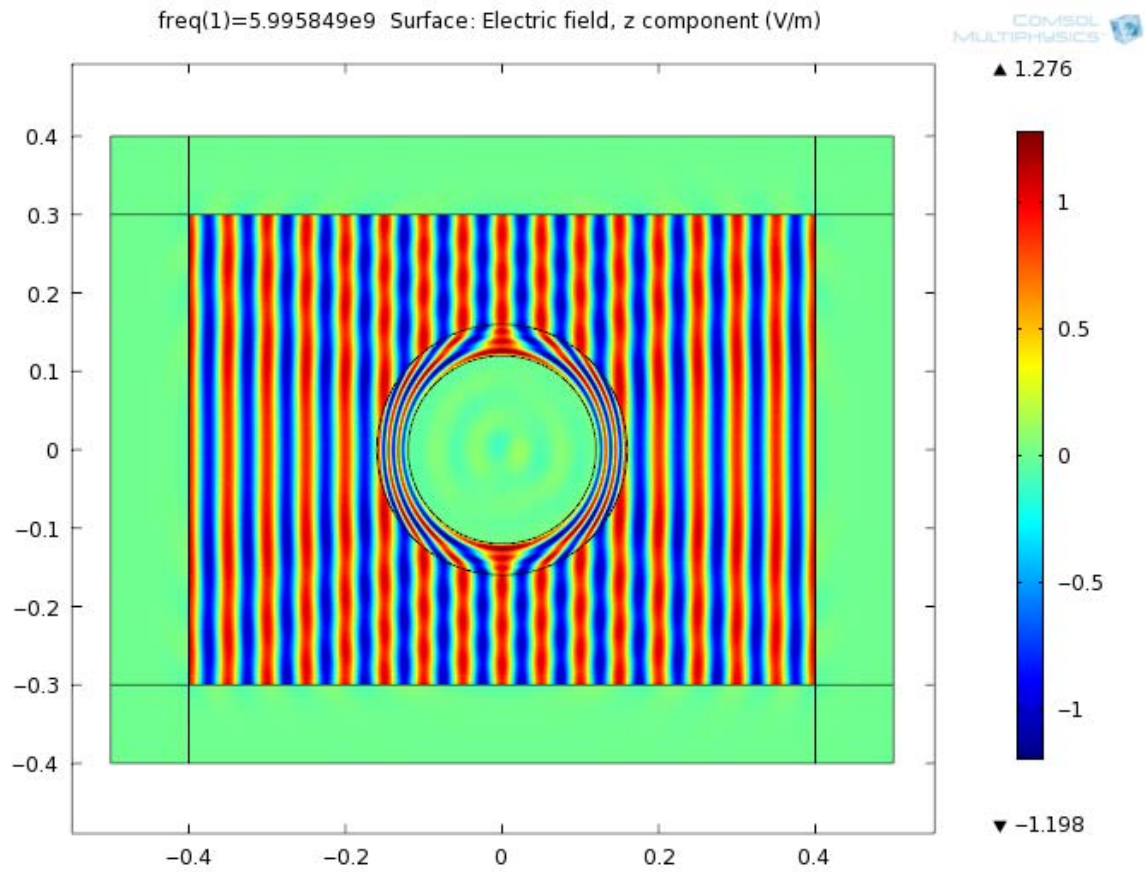
## RESULTS

21. Click on the **Results** tab. Under the **2D Plot Group 1** tab click on **Surface 1**. In the **Expression** field one can look at the Background Field (emw.Ebz) or the Scattered Field (emw.Ez). The following figures were created using this tutorial.

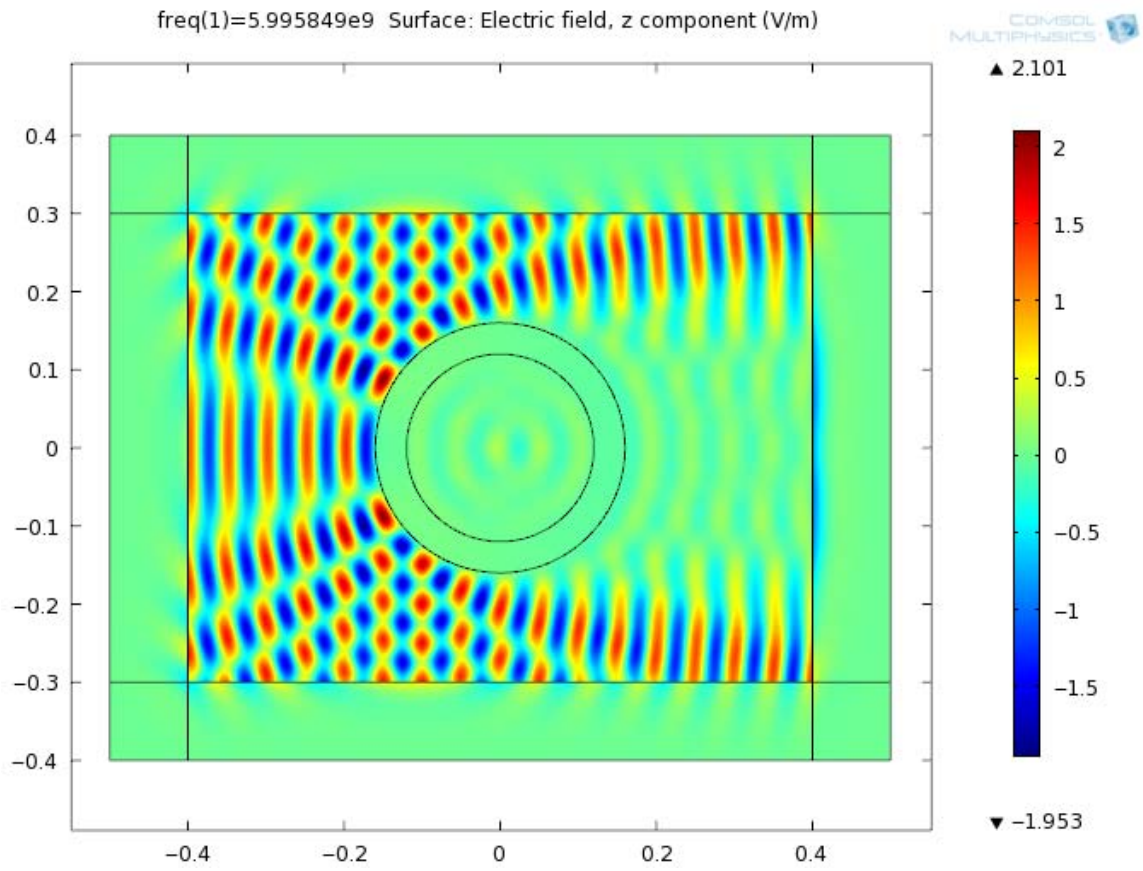
## Incident Electric Field



## Electric Field with Cloaking Material Solution



## Electric Field with Isotropic Material Solution



THIS PAGE IS INTENTIONALLY LEFT BLANK

## LIST OF REFERENCES

- [1] Jefferson Lab, "The FEL Program at Jefferson Lab," <http://www.jlab.org/FEL/> (last accessed 28 July 2010).
- [2] Office of Naval Research, "Directed Energy Program," <http://www.onr.navy.mil/Science-Technology/Departments/Code-35/All-Programs/air-warfare-352/Directed-Energy.aspx> (last accessed 28 July 2010).
- [3] Office of Naval Research, "Free Electron Laser," <http://www.onr.navy.mil/Media-Center/Fact-Sheets/Free-Electron-Laser.aspx> (last accessed 28 July 2010).
- [4] R. K. Ackerman, "Fleet Defense Eyes Lasers," December 2003, [http://www.afcea.org/signal/articles/templates/SIGNAL\\_Article\\_Template.asp?articleid=55&zoneid=22](http://www.afcea.org/signal/articles/templates/SIGNAL_Article_Template.asp?articleid=55&zoneid=22) (last accessed 29 July 2010).
- [5] Office of Naval Research, "Counter Directed Energy Program," <http://www.onr.navy.mil/en/Science-Technology/Departments/Code-35/All-Programs/aerospace-research-351/Counter-Directed-Energy.aspx> (last accessed 02 August 2010).
- [6] J. B. Pendry, D. Schurig, D. R. Smith, "Controlling Electromagnetic Fields," *Science*, vol. 312, no. 5781, pp. 1780-1782, June 2006.
- [7] J. B. Pendry, "Metamaterials and the Control of Electromagnetic Fields," *Optical Society of America Technical Digest*, 2007.
- [8] O. Hess, "Optics: Farewell to Flatland," *Nature*, vol. 455, no. 7211, pp. 299-300, September 2008.
- [9] P. H. Tichit, B. Kante, A. de Lustrac, "Design of polygonal and elliptical invisibility cloaks," Proceedings of Nato ARW and META08, Marrakesh-Morocco, pp. 120-125, 7-10 May 2008.

- [10] D. Schurig, J. B. Pendry, D. R. Smith, "Calculation of Material Properties and Ray Tracing in Transformation Media," *Optics Express*, vol. 14, no. 21, pp. 9794-9804, October 2006.
- [11] Science, "Supporting Online Material for Controlling Electromagnetic Fields," <http://www.sciencemag.org/cgi/content/full/1125907/DC1> (last accessed 11 August 2010).
- [12] M. Rahm, D. Schurig, D. A. Roberts, S. A. Cummer, D.R. Smith, "Design of Electromagnetic Cloaks and Concentrators Using Form-Invariant Coordinate Transformations of Maxwell's Equations," *Photon. Nanostruct. Fundam. Appl.*, vol. 6, is. 1, pp. 87-95, April 2008.
- [13] J. M. Jouvard, A. Soveja, N. Pierron, "Thermal Modelling of Metal Surface Texturing by Pulsed Laser," Excerpt from the *Proceedings of the COMSOL Users Conference*, Paris, 2006.
- [14] J. Alda, "Laser and Gaussian Beam Prorogation and Transformation," *Encyclopedia of Optical Engineering*, p. 999, 2003.
- [15] Encyclopedia of Laser Physics and Technology, "Gaussian Beams," [http://www.rp-photonics.com/gaussian\\_beams.html](http://www.rp-photonics.com/gaussian_beams.html) (last accessed 20 August 2010).
- [16] Absolute Astronomy, "Gaussian Beam," [http://www.absoluteastronomy.com/topics/Gaussian\\_beam](http://www.absoluteastronomy.com/topics/Gaussian_beam) (last accessed 20 August 2010).
- [17] Wikipedia, "Boeing AGM-84 Harpoon," [http://en.wikipedia.org/wiki/Boeing\\_AGM-84\\_Harpoon](http://en.wikipedia.org/wiki/Boeing_AGM-84_Harpoon) (last accessed 01 September 2010).
- [18] Boeing, "Boeing: Harpoon Overview," <http://www.boeing.com/defense-space/missiles/harpoon/index.htm> (last accessed 01 September 2010).



## INITIAL DISTRIBUTION LIST

1. Defense Technical Information Center  
Ft. Belvoir, VA
2. Dudley Knox Library  
Naval Postgraduate School  
Monterey, CA
3. Professor Andres Larraza  
Naval Postgraduate School  
Monterey, CA
4. Professor Carlos F. Borges  
Naval Postgraduate School  
Monterey, CA
5. Professor James H. Luscombe  
Naval Postgraduate School  
Monterey, CA
6. Professor Brett Borden  
Naval Postgraduate School  
Monterey, CA
7. Professor Clyde L. Scandrett  
Naval Postgraduate School  
Monterey, CA
8. LT Alex B. Baynes  
Naval Postgraduate School  
Monterey, CA